Geochemical evidence for a magmatic contribution to the metal budget of the Windy Craggy Cu-Co(±Zn) volcanogenic massive-sulfide deposit, northwestern British Columbia

M.I. Leybourne[1, 2*], J.M. Peter[3], M.A. Schmidt[1], D. Layton-Matthews[1], A. Voinot[1, 2], and L. Mathieu[4]

Leybourne, M.I., Peter, J.M., Schmidt, M.A., Layton-Matthews, D., Voinot, A., and Mathieu, L., 2022. Geochemical evidence for a magmatic contribution to the metal budget of the Windy Craggy Cu-Co(±Zn) volcanogenic massive-sulfide deposit, northwestern British Columbia; in *Targeted Geoscience Initiative 5: volcanic- and sediment-hosted massive-sulfide deposit genesis and exploration methods, (ed.) J.M. Peter and M.G. Gadd; Geological Survey of Canada, Bulletin 617, p. 287–312. https://doi.org/10.4095/328018*

Abstract: Volcanogenic massive-sulfide (VMS) deposits may have had metal contributions from magmatic degassing and leaching of footwall rocks. The Windy Craggy Cu-Co-Zn VMS deposit in northwestern British Columbia may include magmatic contributions, based on laser-ablation inductively coupled plasma mass spectrometry (LA-ICP-MS) of fluid inclusions (enriched in Sb, Sn, and Bi) and lithogeochemistry. Sulfide-mineral trace-element abundances in the massive-sulfide orebody, underlying stockwork zone, gold zone, and altered and unaltered mafic rock and argillite were analyzed by LA-ICP-MS. Elevated Au, W, As, Bi, Sb, Se, Te, Tl, Ag, Co, and Mo contents occur within the gold and/or stockwork zones. Increasing 'magmatic metals' with increasing Co/Ni values suggest direct magmatic contribution to the deposit. Covariation of Co with these so-called 'magmatic elements' indicates that it, too, may be of magmatic origin, sourced via fluids exsolved from a crystallizing magma; however, evidence from the composition of rocks and sulfide minerals from Windy Craggy and other VMS deposits suggests that there is probably no meaningful distinction between hydrothermal leaching and direct magmatic contributions and that most — if not all — fluids that form VMS deposits should be termed 'magmatic-hydrothermal'.

Résumé : Les gîtes de sulfures massifs volcanogènes (SMV) peuvent avoir bénéficié de contributions de métaux provenant d'un dégazage magmatique et du lessivage des roches de l'empilement sous-jacent. Le gisement de SMV à minéralisation de Cu-Co-Zn de Windy Craggy, dans le nord-ouest de la Colombie-Britannique, pourrait inclure des contributions magmatiques, selon l'analyse par spectrométrie de masse avec plasma à couplage inductif jumelée à l'ablation par laser (LA-ICP-MS) d'inclusions fluides (enrichies en Sb, Sn et Bi) et la lithogéochimie. À l'aide de l'analyse par LA-ICP-MS, nous avons déterminé les teneurs en éléments traces de minéraux sulfurés présents dans le corps minéralisé de sulfures massifs, la zone de stockwerk sous-jacente, la zone aurifère, les roches mafiques altérées et non altérées et l'argilite. La zone aurifère et/ou la zone de stockwerk présentaient des teneurs élevées en Au, W, As, Bi, Sb, Se, Te, Tl, Ag, Co et Mo. Un accroissement du contenu en « métaux magmatiques » en parallèle avec une augmentation des valeurs du rapport Co/Ni semble indiquer une contribution magmatique directe au gisement. La covariation de Co et de ces prétendus « éléments magmatiques » indique que le Co pourrait lui aussi être d'origine magmatique et proviendrait de fluides d'exsolution d'un magma en voie de cristallisation. Toutefois, les données sur la composition des roches et des minéraux sulfurés du gisement de Windy Craggy et d'autres gisements de SMV semblent indiquer qu'il n'y a probablement pas de distinction importante entre les contributions provenant d'un lessivage hydrothermal et les contributions magmatiques directes, et que la plupart – sinon l'ensemble – des fluides qui forment les gîtes de SMV devraient être qualifiés de fluides « magmatiques-hydrothermaux ».

[1]Queen's Facility for Isotope Research, Department of Geological Sciences and Geological Engineering, Queen's University, 36 Union Street, Kingston, Ontario K7L 3N6
[2]McDonald Institute, Canadian Particle Astrophysics Research Centre, Department of Physics, Engineering Physics & Astronomy, Queen's University, 64 Bader Lane, Kingston, Ontario K7L 3N6
[3]Geological Survey of Canada, 601 Booth Street, Ottawa, Ontario K1A 0E8
[4]Centre d'études sur les Ressources minérales, Département des Sciences appliquées, Université du Québec à Chicoutimi, 555 boul. de l'université, Chicoutimi, Quebec G7H 2B1
*Corresponding author: M.I. Leybourne (email: m.leybourne@queensu.ca)

INTRODUCTION

The Windy Craggy Cu-Co-Au deposit in northwestern British Columbia (Fig. 1) has been the subject of an ongoing study examining a possible direct magmatic fluid contribution to the mineralizing fluids and mineralization. Windy Craggy is the largest Besshi-type volcanogenic massive-sulfide (VMS) deposit in the world and was chosen for this study due to its atypically large size and the atypically high salinity of fluid inclusions in the stockwork (feeder) zones (Peter and Scott, 1999). These attributes were posited to be the result of direct magmatic contribution of metals and volatiles to the mineralizing hydrothermal fluids and mineralization (Peter, 1992). Besshi-type deposits are stratiform deposits characterized by a mineralogy of massive pyrrhotite and/or pyrite with chalcopyrite as the dominant non–Fe-sulfide mineral, minor sphalerite, and rare galena. Copper is the principal economic metal, with lesser Zn, Co, and Ag±Au. Deposits occur primarily in mafic volcanic rocks and deeper water facies including metagraywacke, quartzite, and metapelite. Besshi-type deposits form back-arc basins, rifted continental margins, intracontinental rifts, fore arcs, and sedimented spreading ridges; felsic volcanic rocks are typically absent or rare.

In this paper, we use laser-ablation inductively coupled plasma mass spectrometry (LA-ICP-MS) mapping techniques to investigate pyrite, chalcopyrite, and pyrrhotite chemical compositions as a tool for characterizing magmatic fluid contributions to the Windy Craggy deposit and to corroborate the previously collected data obtained from LA-ICP-MS analysis of fluid inclusions and bulk geochemistry of host rocks (Schmidt et al., 2018, 2019). The use of sulfide chemistry as a tool for determining if there was a magmatic contribution to a mineralizing system has been the focus of many studies (e.g. Butler and Nesbitt, 1999; Soltani Dehnavi et al., 2018; Mathieu, 2019). Pyrite is studied more commonly than other minerals due to its abundance in hydrothermal and magmatic-hydrothermal systems, its capacity to contain high abundances of many trace elements, its relatively well understood crystal chemistry, and the relationship between metal uptake and the chemical composition of the mineralizing fluid (Large et al., 2009; Deditius et al., 2011; Deditius and Reich, 2016; Mukherjee and Large, 2017).

Cobalt is of particular interest in this study due to its strong enrichment within the Windy Craggy deposit relative to other VMS deposit types. Cobalt is generally not reported in grade and tonnage figures for VMS deposits, except for Windy Craggy and deposits in the Outokumpu (Finland) and Ducktown (Tennessee, U.S.A.) districts (Mudd et al., 2013). Windy Craggy has an average Co grade of 0.083 weight per cent (Peter, 1992). No primary Co-bearing phases have been observed within the deposit, except for rare cobaltite (Peter, 1992), suggesting that the Co is hosted within the pyrite, chalcopyrite, and pyrrhotite (Peter and Scott, 1999). Cobalt abundances are characteristically higher in Besshi-type deposits than in other VMS types (Kase and Yamamoto, 1988). Cobalt occurs within pyrite grains in weakly metamorphosed Besshi-type deposits in small, spot-like domains. As metamorphic grade increases, the Co migrates outward, forming a Co-rich region on the outer border of the host pyrite grain (Itoh, 1976).

A more recent study of the recognition of magmatic fluids through pyrite chemistry also investigated Co distribution in a porphyry copper deposit with respect to metamorphic grade, as well as other factors; cobalt was determined to be one of the primary elements mimicking the growth zoning of pyrite, which results in its irregular distribution within the host grains (Mathieu, 2019). It was also determined that Co migrates within the host grain in response to increasing grades of metamorphism greater that greenschist and at amphibolite facies (Mathieu, 2019). Cobalt solubility is temperature dependent and increases in high-temperature fluids (Huston et al., 1995). This high-temperature dependence has been observed in VMS deposits as enrichments of Co and Ni occur in sulfide minerals deposited at high temperatures (approximately 300–350 °C; Keith et al., 2016; Martin et al., 2019).

In this study, we performed LA-ICP-MS analyses of pyrite, chalcopyrite, and pyrrhotite (the primary sulfide phases in the deposit) and integrated these data with whole-rock geochemistry to understand the deportment of metals and metalloids of potential magmatic derivation within sulfide minerals, compare the LA-ICP-MS metal and metalloid abundances in the primary sulfide minerals with their abundances in bulk analyses of host footwall mafic rocks and argillite, and understand the atypical enrichment of Co within the Windy Craggy deposit.

GEOLOGY

The geology of the Windy Craggy deposit has been previously described in detail (Peter, 1992; Peter and Scott, 1999; Schmidt et al., 2018, 2019), and is only summarized here. The deposit is located in extreme northwestern British Columbia, within rocks of the Alexander terrane, one of the largest accreted terranes in the North American Cordillera (Fig. 1; Coney et al., 1980). The terrane is composed of a thick succession of weakly metamorphosed, complexly deformed, Precambrian to Permian basinal and platformal carbonate and clastic rocks with a minor volcanic component. This succession is unconformably overlain by Upper Triassic calcareous, proximal to distal turbidites and a bimodal volcanic suite (Campbell and Dodds, 1979, 1983; MacIntyre, 1984).

The Windy Craggy deposit is hosted in the Late Triassic section commonly referred to as the Tats volcanic complex. The complex has been subdivided into five major units, described in order from base to top (Fig. 2):

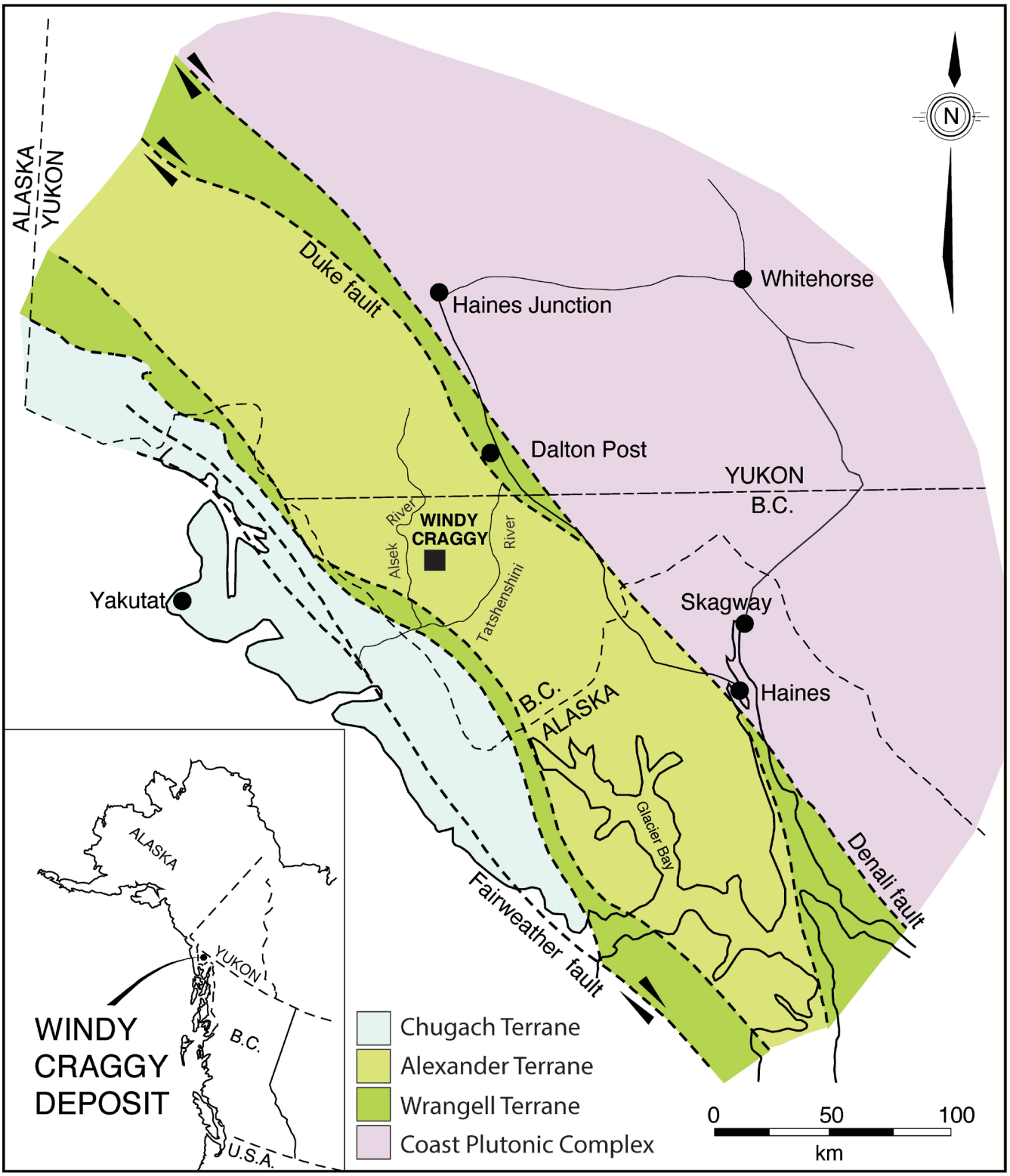

Figure 1. Location and tectonic setting of the Windy Craggy deposit in northwestern British Columbia showing the distribution of the Alexander, Wrangell, and Chugach terranes and the Coast Plutonic Complex (*after* Campbell and Dodds, 1983 and MacIntyre, 1986); *modified from* Peter and Scott (1999).

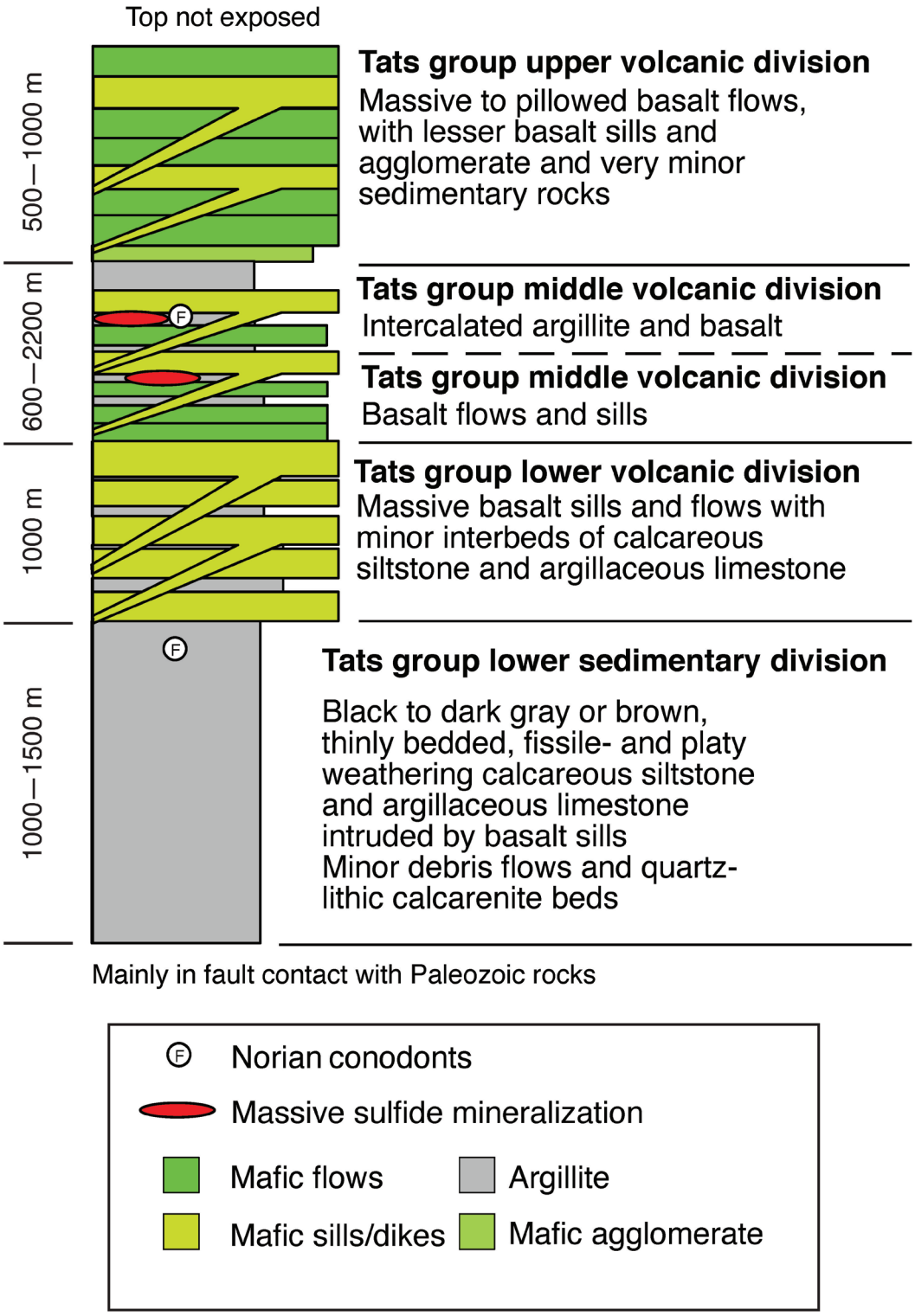

Figure 2. Generalized stratigraphy of the Upper Triassic section of the Alsek-Tatshenshini area, *modified from* Peter and Scott (1999).

1. a grey limestone unit, possibly Silurian to Devonian;
2. a graphitic shale unit, of undefined age, composed of interlayered calcareous and graphitic shale, argillite, and limestone;
3. an approximately 1000 m thick section of Upper Triassic mafic flows and sills, referred to as the Lower Tats;
4. an approximately 2000 m thick section of interbedded graphitic and calcareous argillites, pillowed and massive mafic flows, tuff, agglomerate, and limestone, referred to as the Middle Tats, with Upper Triassic (ca. 225 Ma) conodont assemblages in the limestone (Orchard, 1986); and
5. an uppermost unit composed mostly of an approximately 1000 m thick section of Upper Triassic pillow basalts, referred to as the Upper Tats.

The deposit consists of two main lenses (North sulfide body and South sulfide body), which contain most of the Cu-Co-Au mineralization (Fig. 3). There is also a smaller lens (Ridge sulfide zone) that is located immediately north of the North sulfide body, which was only discovered near the end of the Geddes exploration program in the early 1990s (prior to expropriation and formation of a park in 1993); this Zn-rich mineralization is not considered in the resource estimate (*see* below). Each of the two main lenses is underlain by a moderately to well-developed stockwork zone consisting of pyrite, pyrrhotite, chalcopyrite, quartz, and chlorite veins (Peter and Scott, 1999). The South sulfide body is more deformed than the North sulfide body. Collectively, the sulfide bodies contain greater than 300 000 000 t grading 2.12 weight per cent Cu, 0.083 weight per cent Co, 0.16 g/t Au, and 3.30 g/t Ag (Downing et al., 1990). A particularly gold-rich zone (referred to as the gold zone) at the intersection of two major faults at the northwestern edge of the South sulfide body contains up to 14.7 g/t Au over 29.7 m (Peter and Scott, 1999).

METHODS

Whole-rock geochemistry

We compare the LA-ICP-MS data for sulfide minerals to whole-rock geochemistry from three other data sets, from 1) Peter (1992), where data are reported based on X-ray fluorescence (XRF) for major elements and some trace elements and neutron activation analysis for trace elements; 2) Schmidt et al. (2019), where data are reported based on ICP-MS and optical emission spectroscopy (ICP-OES) following lithium metaborate fusion and four-acid digestion; and 3) Geddes Resources Ltd. (unpub. data, [1989]), who completed bulk assays by modified aqua regia (HNO_3:HCl:H_2O; ACME Analytical, Vancouver, Canada) during their extensive 1988 drilling campaign (approximately 3500 analyses that included Mo, Cu, Pb, Zn, Ag, Ni, Co, Mn, Fe, As, U, Au, Th, Sr, Cd, Sb, Bi, V, Ca, P, La, Cr, Mg, Ba, Ti, B, Al, Na, K, and W). One standard was measured throughout the Geddes analyses ('standard C') for a total of 107 analyses. Most relative standard deviation (RSD) values are less than 10% (with the exception of U = 13.3% and Na = 10.24%). Elements used in this study have the following RSD values: Cu = 3.67%, Pb = 5.78%, Zn = 1.33%, Ni = 3.07%, Co = 4.27%, Fe = 2.68%, and Mg = 3.46%. Given that these are aqua regia digestion results, these RSD values are excellent.

Sulfide mineral samples for LA-ICP-MS

Representative samples for LA-ICP-MS were selected from throughout the deposit to obtain a detailed understanding of how the trace-element chemistry of pyrite, chalcopyrite, and pyrrhotite varies throughout the deposit. These samples encompass the footwall, stockwork, massive sulfide, and gold zone regions and include altered and unaltered mafic rock and argillite (Table 1, 2). Polished thin sections were imaged using an Olympus® camera attached to a conventional reflected-light petrographic microscope prior to analysis. Additional imaging was performed using an FEI Quanta field-emission gun scanning electron microscope at the Queen's Facility for Isotope Research (QFIR).

Quantitative LA-ICP-MS analyses were conducted at QFIR using an ESI-NWR 193 nm Excimer ArF laser coupled to a Thermo-Finnigan X-Series II Quadrupole ICP-MS. The parameters used for these analyses were: a beam size of 20 µm, a laser frequency of 10 Hz, fluence of 7.5 to 8 J/cm^2, and an energy density of 100%. Four certified reference materials were used: NIST 610, NIST 612, NIST 614 (Jochum et al., 2011), and MASS-1 (Wilson et al., 2002). These were analyzed using lines with a beam size of 20 µm and a scan speed of 10 µm. The grain analyses were performed in a mapping configuration (beam rastering) with an offset equal to that of the beam size.

Data processing for LA-ICP-MS

Data reduction and map production were done using iolite version 3 (Paton et al., 2011). Data were reduced using the trace-element data reduction scheme in semi-quantitative mode and quantified by stoichiometry using Fe. MASS-1 was used as the standard reference material. The maps produced using iolite were further examined and characterized using Monocle (Petrus et al., 2017). Regions of interest (ROI) were selected to include entire pyrite, chalcopyrite, and pyrrhotite grains to provide an average composition of the individual grain. Each ROI was corrected stoichiometrically by multiplying each channel by the ratio of expected Fe over measured Fe, similar to other studies (e.g. Petrus et al., 2017).

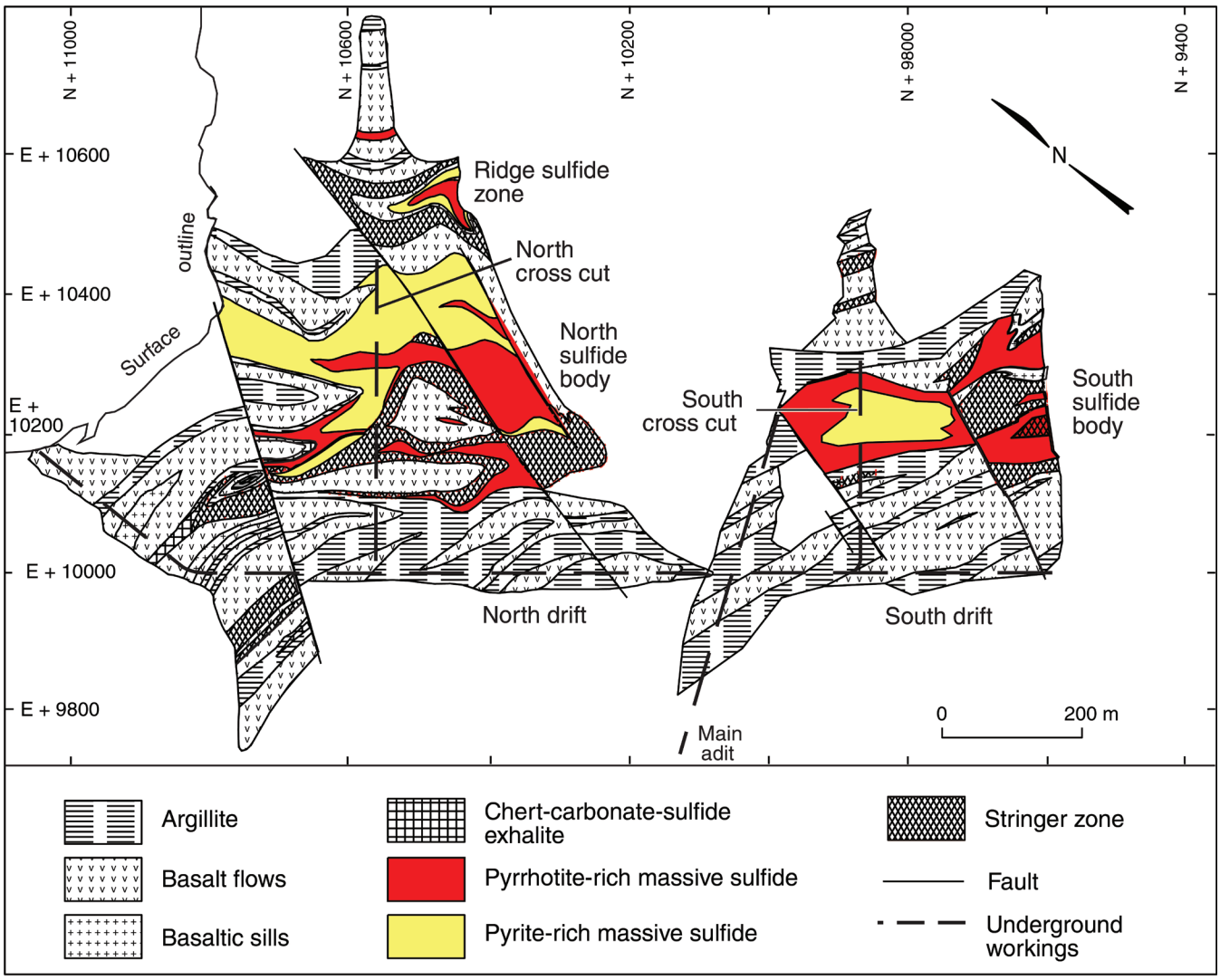

Figure 3. Plan of the 1400 m level (exploration adit level) of the Windy Craggy deposit, northwestern British Columbia, showing the explored, drilled, and developed portions *after* Geddes Resources Ltd. (unpub. rept., 1990), *modified from* Peter and Scott (1999).

RESULTS

Geochemistry of Windy Craggy footwall rocks and ores

During the height of exploration of the Windy Craggy deposit, Geddes Resources Ltd. drilled a large number of holes and completed approximately 3500 multi-element analyses of drill core by modified aqua regia; selected plots of these data are shown in Figures 4 and 5. We compared these data to the whole-rock data of Peter (1992) and the data of Schmidt et al. (2019). There are some notable differences between the three data sets: 1) the number of analyses (approximately 3500 versus <100); 2) the Geddes analyses use aqua regia digestion, whereas the other data sets are 'whole rock' (e.g. XRF, fusion ICP, and four-acid digestion (which can be considered to be 'total', or 'near total' in the case of four acid)); 3) the whole-rock data sets (Peter, 1992; Schmidt et al., 2019) can be subdivided on the basis of rock type, whereas the Geddes data represent 2 m core interval assays, without regard for rock type or extent of alteration. For many elements it is difficult to impossible to compare whole-rock (total) abundances with those determined using aqua regia digestion. Aqua regia is efficient at dissolving carbonate, sulfide, and some oxide minerals, but generally does not digest silicates, except where most particles are less than 2 μm (e.g. Church et al., 1987).

Although we have no way to directly compare the aqua regia and whole-rock data for most elements in this study, we do have a data set of fusion, four-acid (Volesky et al., 2017), and aqua regia (Leybourne, unpub. data, 2020) results on the same samples. These samples are from a variably altered and metamorphosed gossan/VMS deposit and related felsic, mafic, and metasedimentary rocks. These data

Table 1. Location data for samples of sulfide minerals from the Windy Craggy deposit, northwestern British Columbia.

WC Sample #	Description	Section	Azimuth (°)	Dip (°)	Length (m)	Collar elevation (m)	UTM (NAD 83, zone 8)		Sulfide body	Mineral
							Northing	Easting		
88-43-333.4	Argillite	9910N	51.63	16.37	358.50	1394.45	6624253.06	345591.41	SSB	Py
88-43-333.4	Argillite	9910N	51.63	16.37	358.50	1394.45	6624253.06	345591.41	SSB	Py
88-43-333.4	Argillite	9910N	51.63	16.37	358.50	1394.45	6624253.06	345591.41	SSB	Py
88-43-333.4	Argillite	9910N	51.63	16.37	358.50	1394.45	6624253.06	345591.41	SSB	Cp
88-24-306	Argillite	10000N	49.00	36.18	333.76	1395.94	6624322.27	345534.05	SSB	Py
88-43-333.4	Argillite	9910N	51.63	16.37	358.50	1394.45	6624253.06	345591.41	SSB	Py
88-43-333.4	Argillite	9910N	51.63	16.37	358.50	1394.45	6624253.06	345591.41	SSB	Py
88-43-333.4	Argillite	9910N	51.63	16.37	358.50	1394.45	6624253.06	345591.41	SSB	Py
88-23-036.2	Argillite in stockwork	10730N north face	—	—	—	—	—	—	N face	Cp
88-23-036.2	Argillite in stockwork	10730N north face	—	—	—	—	—	—	N face	Po
88-24-312.45	Exhalite	10000N	49.00	36.18	333.76	1395.94	6624322.27	345534.05	SSB	Py
88-50-144.95	Gold zone	10000N main adit	297.42	89.65	181.05	1398.17	6624441.27	345673.28	SSB	Po
88-50-144.95	Gold zone	10000N main adit	297.42	89.65	181.05	1398.17	6624441.27	345673.28	SSB	Cp
88-50-144.95	Gold zone	10000N main adit	297.42	89.65	181.05	1398.17	6624441.27	345673.28	SSB	Cp
88-50-144.95	Gold zone	10000N main adit	297.42	89.65	181.05	1398.17	6624441.27	345673.28	SSB	Py
88-41-300	Massive sulfide	9910N	51.47	17.93	341.38	1395.53	6624253.15	345514.00	SSB	Py
88-41-300	Massive sulfide	9910N	51.47	17.93	341.38	1395.53	6624253.15	345514.00	SSB	Py
88-41-300	Massive sulfide	9910N	51.47	17.93	341.38	1395.53	6624253.15	345514.00	SSB	Po
88-41-300	Massive sulfide	9910N	51.47	17.93	341.38	1395.53	6624253.15	345514.00	SSB	Cp

include 33 samples for which we have aqua regia results and four-acid and/or fusion data for many elements, including Mg, Al, Fe, Mn, Cr, Ni, Co, Cu, Zn, and Zr. The slope of the line between aqua regia and total digestions is variable, ranging from 1.0 for Cu to 0.05 for Zr. For other key elements, the slopes are Mg = 0.96, Fe = 0.78, Al = 0.40, Cr = 0.87, Co = 0.93, Ni = 0.88, and Zn = 0.87. Of these elements, we only have total and aqua regia data for Cu, Ni, and Co in the data presented by Schmidt et al. (2019); for these the slopes are Co = 0.95 ($r = 0.996$, $p < 0.0001$, $n = 15$), Ni = 0.99 ($r = 0.999$, $p < 0.0001$, $n = 15$), and Cu = 1.00 ($r = 0.999$, $p < 0.0001$, $n = 9$). On the basis of these results, Figures 4 and 5 show the differences between the Geddes geochemical data and the whole-rock data for a small number of analytes, with the caveat that we are interested in broad-scale differences between the behaviours of Fe, Mg, Ni, Cr, Co, and Al in these data sets.

The Geddes and whole-rock data demonstrate both a typical fractionation trend for mafic rocks (decreasing Cr and Ni with decreasing Mg; *see* Fig. 4c, d and Fig. 5e, f for Ni) and the effects of the addition of Fe by the mineralizing fluids, with Fe up to approximately 50 weight per cent in the Geddes aqua regia analyses (Fig. 4a). Because the host volcanic rocks (flows and tuffs) and intrusive rocks (sills and dykes) are alkalic (Peter et al., 2014), there should be limited Fe enrichment as a result of typical igneous fractionation (i.e. minimal enrichment in Fe with decreasing Mg for mafic rocks at Windy Craggy; Fig. 4b). As Fe increases above

Table 1. (cont.) Location data for samples of sulfide minerals from the Windy Craggy deposit, northwestern British Columbia.

WC Sample #	Description	Section	Azimuth (°)	Dip (°)	Length (m)	Collar elevation (m)	UTM (NAD 83, zone 8)		Sulfide body	Mineral
							Northing	Easting		
88-41-300	Massive sulfide	9910N	51.47	17.93	341.38	1395.53	6624253.15	345514.00	SSB	Cp
88-41-300	Massive sulfide	9910N	51.47	17.93	341.38	1395.53	6624253.15	345514.00	SSB	Py
WCU89-42	Stockwork/ stringer	Underground	—	—	—	—	—	—	NSB	Py
90-157-215	Volcanic flow	—	—	—	—	1396.00	6624400.00	345514.00	NSB	Po
90-157-215	Volcanic flow	—	—	—	—	1396.00	6624400.00	345514.00	NSB	Cp
88-54-073.3	Volcanic tuff	10327N	49.47	0.30	320.04	1394.57	6624574.05	345323.74	NSB	Po
88-42-135.2	Volcanic tuff	10268N	46.60	59.68	403.30	1396.75	6624528.79	345360.78	NSB	Cp
88-42-135.2	Volcanic tuff	10268N	46.60	59.68	403.30	1396.75	6624528.79	345360.78	NSB	Cp
88-42-135.2	Volcanic tuff	10268N	46.60	59.68	403.30	1396.75	6624528.79	345360.78	NSB	Po
88-42-135.2	Volcanic tuff	10268N	46.60	59.68	403.30	1396.75	6624528.79	345360.78	NSB	Cp
88-42-135.2	Volcanic tuff	10268N	46.60	59.68	403.30	1396.75	6624528.79	345360.78	NSB	Cp
88-42-135.2	Volcanic tuff	10268N	46.60	59.68	403.30	1396.75	6624528.79	345360.78	NSB	Po
88-42-135.2	Volcanic tuff	10268N	46.60	59.68	403.30	1396.75	6624528.79	345360.78	NSB	Po
88-46-093.8	Volcanic tuff	10327N	49.18	45.23	396.24	1396.92	6624574.07	345323.21	NSB	Po
88-46-093.8	Volcanic tuff	10327N	49.18	45.23	396.24	1396.92	6624574.07	345323.21	NSB	Py
88-46-093.8	Volcanic tuff	10327N	49.18	45.23	396.24	1396.92	6624574.07	345323.21	NSB	Po
88-28-249	Volcanic tuff (footwall)	10030N	51.12	46.83	329.12	1396.42	6624345.61	345514.75	SSB	Py
88-28-249	Volcanic tuff (footwall)	10030N	51.12	46.83	329.12	1396.42	6624345.61	345514.75	SSB	Py

Abbreviations: Cp: Chalcopyrite; Po: pyrrhotite; Py: pyrite; SSB: South sulfide body; N: north; NSB: North sulfide body

approximately 20 weight per cent and Mg decreases below approximately 1 weight per cent, Cu increases dramatically, up to approximately 7000 ppm (Fig. 4a). Similarly, as Cu increases in the Geddes data, both Ni and Cr decrease (Fig. 4c); trends of decreasing Ni and Cr are also evident in the whole-rock data, although five mafic flow samples show anomalously high Ni (these have high loss-on-ignition and CO_2; Fig. 4d).

As Mg decreases owing to fractionation in mafic magmatic systems, Al typically increases, as shown by the whole-rock mafic volcanic and intrusive rock data, whereas for the assay data, Al decreases to near zero as Mg decreases to less than 1 weight per cent (cf. Fig. 5a, b). Whole-rock data for argillite and massive-sulfide samples show a similar decrease in Al with decreasing Mg (Fig. 5b), as shown by the Geddes geochemical data (Fig. 5a). Typically, as mafic magmas fractionate, compatible transition metals decrease as Mg decreases; Cr, Ni, Co, V, and, to a lesser extent, Sc are variably incorporated into early-formed mineral phases (olivine, clinopyroxene); this is because these metals typically have mineral-melt distribution coefficients greater than 1 (Villemant et al., 1981). For the Windy Craggy whole-rock data, Co and Ni decrease with decreasing Mg (Fig. 5d, f, respectively). By contrast, for the Geddes analytical data, although Ni also decreases with decreasing Mg (and increasing Cu; Fig. 5e), Co increases to between approximately 100 and greater than 1000 ppm at Mg contents less than 1 weight per cent; Fig. 5c). Thus, as Fe and Cu

Table 2. Laser-ablation inductively coupled plasma mass spectrometry trace-element (and Cu) data for sulfide mineral samples from the Windy Craggy deposit, northwestern British Columbia.

WC Sample #	Mineral	Cu (wt %)	V (ppm)	Cr (ppm)	Mn (ppm)	Co (ppm)	Ni (ppm)	Zn (ppm)	Ga (ppm)	Ge (ppm)	As (ppm)	Se (ppm)	Mo (ppm)	Ag (ppm)	Cd (ppm)
88-43-333.4	Py	0.59	0.037	0.043	46.34	47.68	45.44	13716	0.30	0.40	229	31.37	0.38	18.44	0.001
88-43-333.4	Py	0.14	0.034	0.14	79.36	367.11	19.21	893	0.13	0.22	366	13.35	0.26	126	0.001
88-43-333.4	Py	0.026	0.035	0.090	43.91	98.10	18.06	68.26	0.48	0.094	249	17.94	0.007	4.12	0.002
88-43-333.4	Cp	32.70	5.01	0.12	329	0.62	2.05	3054	1.22	0.13	6	43.16	0.17	213	11.98
88-24-306	Py	0.000	9.01	2.62	8669	29.86	36.61	14.30	0.52	1.18	0.15	0.87	0.24	1.19	0.13
88-43-333.4	Py	0.011	0.79	0.98	15.51	601	52.95	3383	0.15	0.85	1905	0.21	0.051	0.013	5.21
88-43-333.4	Py	0.012	0.78	1.38	16.04	669	64.07	221	0.12	0.87	5024	0.22	2.68	38.60	0.72
88-43-333.4	Py	0.24	1.42	1.28	194.08	172	109.12	4905	1.59	0.62	234	4.88	0.15	50.29	9.77
88-23-036.2	Cp	0.91	718	12.33	7498	3.28	3.43	1762	70.24	21.92	25.46	18.98	215	112	25.98
88-23-036.2	Po	0.003	8.22	0.33	436	0.42	8.46	157	1.48	5.53	2.70	21.31	0.45	25.08	7.92
88-24-312.45	Py	0.041	0.49	0.15	23.97	324	11.92	54.44	0.11	0.50	305	0.76	3.78	4.60	0.40
88-50-144.95	Po	0.046	0.035	0.020	115.11	678	0.016	31.74	0.050	1.11	0.002	0.024	1.68	2.05	0.000
88-50-144.95	Cp	34.33	0.64	0.13	29.43	0.83	0.34	6965	3.66	2.88	0.43	6.90	2.10	346	148
88-50-144.95	Cp	34.62	0.53	0.13	35.16	0.69	0.31	6970	3.54	2.55	0.35	6.34	2.19	319	139
88-50-144.95	Py	0.027	0.18	0.074	6.02	274	7.52	58.92	0.22	3.36	12.97	4.43	7.88	20.57	1.85
88-41-300	Py	0.051	0.045	0.052	3.69	582	3.80	13.43	1.02	0.018	33.71	6.41	0.009	0.53	0.37
88-41-300	Py	0.057	1.46	0.053	23.81	859	5.72	78.99	0.79	0.018	113	7.81	0.010	0.81	0.51
88-41-300	Po	0.018	0.019	0.28	36.43	272	0.084	21.51	0.004	1.60	0.011	2.31	2.86	0.20	0.001
88-41-300	Cp	40.86	0.25	0.29	12.67	1281	11.81	767	0.051	2.35	0.14	36.10	3.80	4.13	6.91
88-41-300	Cp	27.65	0.18	0.37	119.67	1292	0.81	418	0.11	0.38	71.07	7.79	2.14	1.51	0.76
88-41-300	Py	0.24	0.17	0.13	84.36	1640	0.86	196	0.064	0.28	226	2.43	6.89	3.05	0.15
WCU89-42	Py	0.023	26.93	0.31	3.61	3921	205.19	37.60	7.03	2.85	1077	20.85	0.076	7.85	0.000
90-157-215	Po	4.02	12.67	3.30	961	206	52.21	133	0.037	0.43	3.79	6.77	0.72	1.35	0.73
90-157-215	Cp	33.56	7.37	1.93	217	11.29	6.43	1734	1.85	0.12	3.22	7.60	0.41	2.65	2.79
88-54-073.3	Po	0.008	2.22	0.99	85.99	1499	492	92.11	0.55	4.06	73.15	85.78	1.49	3.75	1.24
88-42-135.2	Cp	32.04	0.88	1.07	5366	25.65	15.96	964	0.20	0.78	0.18	13.77	0.086	20.84	5.14
88-42-135.2	Cp	34.14	0.71	0.51	696	5.39	6.22	1054	0.039	0.53	0.30	11.45	0.040	22.12	0.95
88-42-135.2	Po	0.006	30.71	4.94	69845	5.38	2.85	41.02	0.29	1.13	1.03	1.30	0.67	0.15	0.053
88-42-135.2	Cp	41.93	2.48	2.83	892	28.62	8.96	1437	0.29	0.26	0.067	13.03	0.18	32.10	11.15
88-42-135.2	Cp	40.10	1.87	1.44	622	14.03	7.71	1415	0.25	0.86	0.067	14.59	0.13	41.71	12.53
88-42-135.2	Po	0.003	76.46	11.32	87300	6.42	2.56	76.15	1.37	1.46	0.22	3.95	0.30	0.098	0.004
88-42-135.2	Po	0.013	69.23	10.95	107536	10.96	2.21	80.54	0.60	1.38	0.87	1.80	0.45	0.19	0.004
88-46-093.8	Po	0.014	140.17	69.16	2319	37.28	259	184	5.60	3.92	0.74	35.10	3.29	0.41	0.23
88-46-093.8	Py	0.012	8.15	30.01	217	76.49	412	53.41	0.54	0.34	0.98	55.03	10.64	1.28	0.005
88-46-093.8	Po	0.017	63.11	19.77	31060	34.23	234	128	2.34	2.86	0.16	19.95	1.28	0.37	0.009
88-28-249	Py	0.047	321	116	126271	771	2287	652	14.74	4.36	3.11	13.40	1.34	2.75	5.73
88-28-249	Py	0.003	69.58	243	7124	1689	4943	141	5.54	0.46	0.15	7.95	0.027	1.57	0.004

Table 2 (cont.). Laser-ablation inductively coupled plasma mass spectrometry trace-element (and Cu) data for sulfide mineral samples from the Windy Craggy deposit, northwestern British Columbia.

WC Sample #	Mineral	In (ppm)	Sn (ppm)	Sb (ppm)	Te (ppm)	Ba (ppm)	W (ppm)	Au (ppm)	Hg (ppm)	Tl (ppm)	Pb (ppm)	Bi (ppm)	Ir (ppm)	Pt (ppm)	Co/Ni
88-43-333.4	Py	0.31	0.56	1.90	0.066	0.94	0.011	0.009	0.098	0.044	16.57	0.029	11.77	38.82	1.05
88-43-333.4	Py	0.054	0.38	2.27	0.080	1.58	0.078	0.020	0.089	0.063	19.24	0.033	19.26	98.15	19.11
88-43-333.4	Py	0.069	0.22	2.32	0.017	6.17	0.020	0.041	0.092	0.035	14.17	0.022	27.99	77.58	5.43
88-43-333.4	Cp	2.94	8.07	2.29	0.19	4.38	0.45	0.072	0.27	0.18	32.03	0.020	1.12	92.80	0.31
88-24-306	Py	0.034	1.40	0.77	0.19	0.017	3.91	0.035	0.36	0.29	25.13	0.075	8.43	57.71	0.82
88-43-333.4	Py	0.033	6.36	2.06	0.31	1.33	0.097	0.093	2.16	0.30	53.62	0.034	0.37	8.93	11.35
88-43-333.4	Py	0.016	0.36	1.46	0.16	0.89	0.037	0.27	3.13	0.24	26.75	0.009	15.19	43.08	10.45
88-43-333.4	Py	0.070	0.33	1.09	0.098	1.01	0.024	0.11	21.31	0.087	33.23	0.014	3.32	9.36	1.58
88-23-036.2	Cp	1.65	109.89	12.18	0.004	0.051	690	2.46	0.022	5.16	36.00	0.40	0.095	–0.083	0.96
88-23-036.2	Po	0.001	2.45	4.41	0.004	0.003	0.69	0.57	0.021	4.89	18.45	0.27	0.087	–0.073	0.05
88-24-312.45	Py	0.040	0.55	13.71	1.72	0.005	0.27	4.16	3.20	2.11	111	0.20	8.31	15.95	27.20
88-50-144.95	Po	0.005	1.49	3.09	0.18	0.017	0.19	1.40	25.09	0.001	9.80	2.31	1.77	526	41613
88-50-144.95	Cp	9.45	104.65	19.55	0.86	0.002	0.37	7.12	3328	142	15.02	0.13	0.062	0.20	2.46
88-50-144.95	Cp	9.65	108.73	17.80	0.92	0.001	0.26	6.34	3283	127	13.28	0.20	0.063	0.20	2.23
88-50-144.95	Py	0.037	1.66	11.15	0.72	0.001	0.75	1.77	60.31	23.52	3.52	5.91	0.028	0.089	36.48
88-41-300	Py	0.027	0.11	2.45	0.022	0.86	0.013	0.067	7.39	0.15	11.73	0.56	26.96	90.97	153
88-41-300	Py	0.005	0.11	12.42	0.022	3.21	3.61	0.067	11.81	0.46	52.91	0.50	16.58	1.62	150
88-41-300	Po	0.002	1.00	0.011	3.82	0.050	0.006	0.001	1.36	0.14	9.62	0.001	0.43	7.37	3241
88-41-300	Cp	0.028	18.50	0.15	4.16	0.22	0.34	0.13	280	0.26	16.77	0.016	88.87	78.65	108
88-41-300	Cp	0.36	4.74	1.10	6.22	0.33	0.19	0.088	152	2.61	63.74	1.19	5.87	6.55	1601
88-41-300	Py	0.062	0.37	3.10	16.16	0.091	0.52	0.13	11.14	9.03	92.35	1.76	2.73	17.81	1909
WCU89-42	Py	0.036	0.53	27.71	93.99	0.003	1.84	2.51	18.67	7.01	16.07	9.55	0.018	0.056	19.11
90-157-215	Po	1.52	1.25	0.22	0.61	0.60	0.35	0.15	30.88	0.26	20.42	0.098	14.26	73.30	3.94
90-157-215	Cp	11.60	5.48	0.38	1.77	0.33	0.53	0.17	140.42	0.24	13.01	0.067	19.16	97.93	1.76
88-54-073.3	Po	0.004	1.19	0.54	4.68	0.29	0.32	0.12	110	0.47	28.08	0.33	11.17	334	3.04
88-42-135.2	Cp	9.94	25.73	1.19	2.06	1.56	0.031	0.042	10.61	0.47	11.94	0.081	1.20	3.78	1.61
88-42-135.2	Cp	9.54	25.27	0.90	1.45	0.37	0.064	0.003	16.33	0.40	6.70	0.053	1.08	3.40	0.87
88-42-135.2	Po	0.84	0.72	0.64	0.12	1.34	0.91	0.014	0.77	0.10	22.40	0.031	12.15	21.20	1.89
88-42-135.2	Cp	11.30	38.22	1.33	1.79	0.015	0.035	0.020	0.32	0.58	23.25	0.17	1.33	4.19	3.19
88-42-135.2	Cp	13.32	46.95	1.90	1.88	0.015	0.19	0.014	0.32	1.03	25.02	0.19	1.34	4.20	1.82
88-42-135.2	Po	1.03	1.02	0.18	0.12	5.35	1.09	0.004	1.88	0.036	11.86	0.016	1.37	4.29	2.50
88-42-135.2	Po	1.10	1.35	0.56	0.067	0.017	0.92	0.009	0.37	0.059	10.45	0.084	1.55	4.88	4.96
88-46-093.8	Po	0.22	50.22	2.00	0.45	1047.57	1.22	0.009	0.79	1.14	31.93	0.36	3.32	145	0.14
88-46-093.8	Py	0.14	47.76	2.57	1.20	43.80	0.40	0.12	0.42	1.69	33.05	0.79	1.78	5.59	0.19
88-46-093.8	Po	0.17	44.89	1.76	0.13	725.13	2.24	0.20	1.44	0.83	40.77	0.23	3.04	9.55	0.15
88-28-249	Py	1.34	5.72	0.87	1.63	102	1.19	0.21	2.46	0.52	84.72	0.21	152	411	0.34
88-28-249	Py	0.12	0.61	0.61	0.062	5.03	1.53	0.22	1.11	0.12	25.08	0.25	1.43	4.49	0.34

Abbreviations: Cp: Chalcopyrite; Po: pyrrhotite; Py: pyrite; ppm: parts per million; ppb: parts per billion

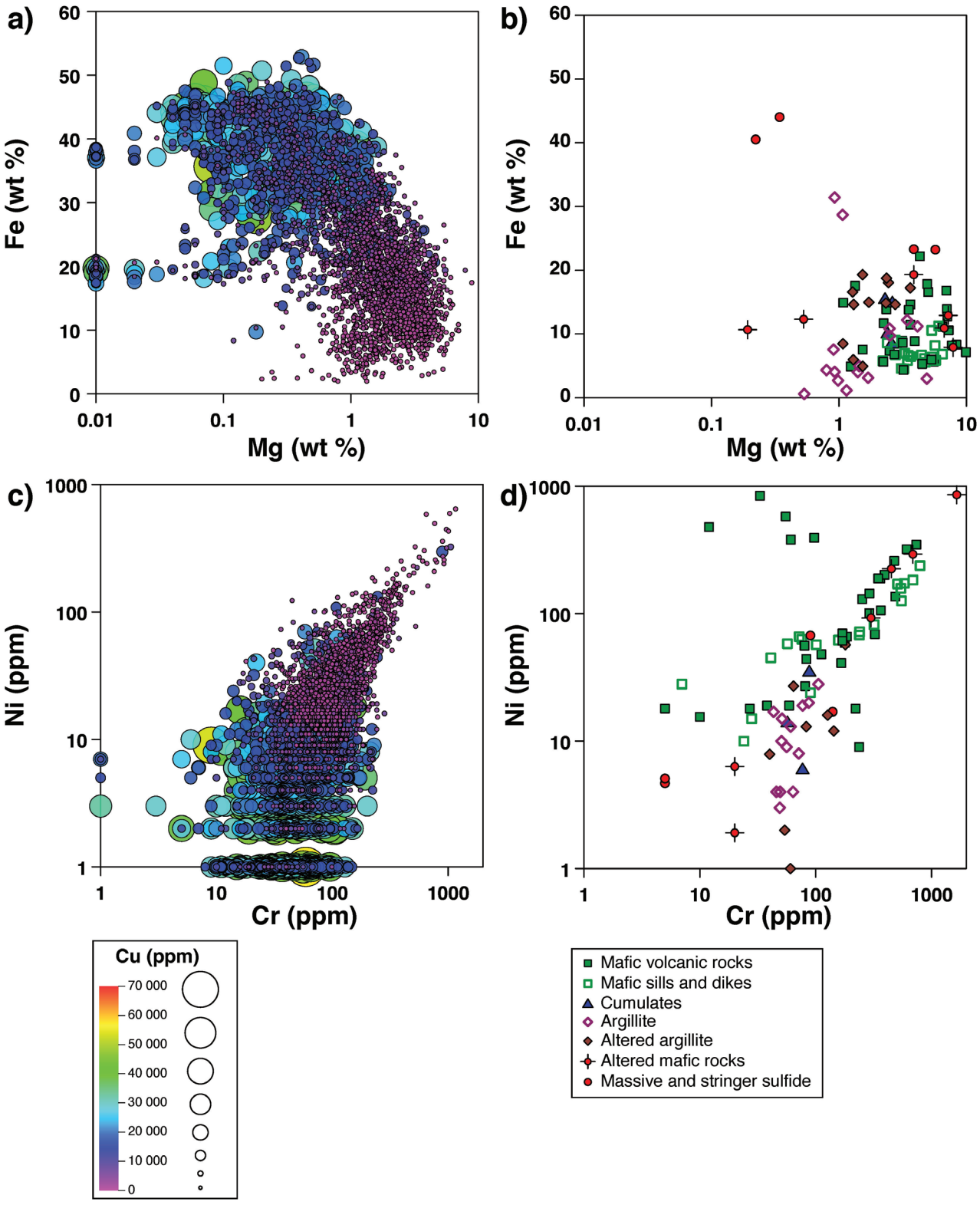

Figure 4. Plots of aqua regia (*after* Geddes Resources Ltd., unpub. rept., 1990) and whole-rock geochemistry data (*after* Schmidt et al., 2019) from the Windy Craggy deposit, northwestern British Columbia: **a)** Cu abundance with respect to Fe and Mg abundances; **b)** Fe versus Mg for various rock types; **c)** Cu abundance with respect to Ni and Cr abundances; and **d)** Ni versus Cr for various rock types.

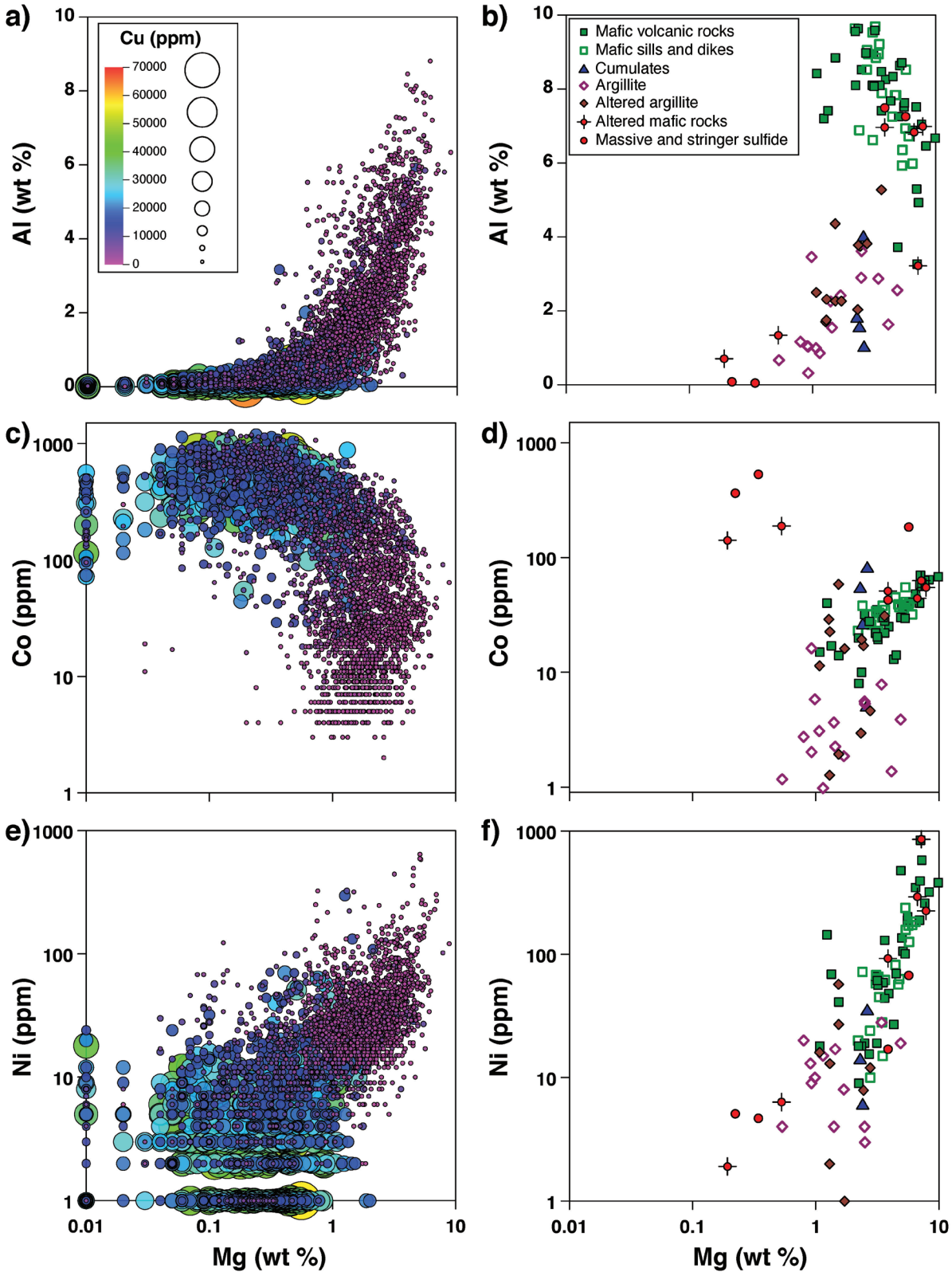

Figure 5. Plots of aqua regia (*after* Geddes Resources Ltd., unpub. rept., 1990) and whole-rock geochemistry data (*after* Schmidt et al., 2019) from the Windy Craggy deposit, northwestern British Columbia: **a)** Cu abundance with respect to Al and Mg abundances; **b)** Al versus Mg for various rock types; **c)** Cu abundance with respect to Co and Mg abundances; **d)** Co versus Mg for various rock types; **e)** Cu abundance with respect to Ni and Mg abundances; and **f)** Ni versus Mg for various rock types.

were added to the rocks during mineralization, Al, Ni, and Mg decreased, whereas Co increased (Fig. 5). This decrease in Ni and increase in Co as Mg decreases is reflected in the large variation of Co/Ni values (<0.1 to approximately 1000) shown by the aqua regia and whole-rock data (Fig. 6).

A number of studies have reported the variation in Co/Ni values in pyrite (and more rarely, other sulfide minerals) as an indicator of the origin of pyrite, with a Co/Ni value of less than 1 commonly ascribed to pyrite of sedimentary origin (Loftus-Hills and Solomon, 1967; Bralia et al., 1979; Bajwah et al., 1987) or in magmatic Ni-Cu deposits (Bajwah et al., 1987), values from 1 to 10 indicating hydrothermal pyrite, and values much greater than this indicative of hydrothermal pyrite from mafic and ultramafic source rocks (Bajwah et al., 1987; Nimis et al., 2008). Given the generally high degree of recovery for Co and Ni by aqua regia compared to four-acid and fusion digestions, comparison of the behaviour of metals in the different sample types to Co/Ni values is broadly appropriate (Fig. 6). Comparison of the three data sets (Geddes aqua regia, whole rock, and LA-ICP-MS of sulfide minerals) shows that both the whole-rock and Geddes aqua regia geochemical data have increasing Cu, Bi (notwithstanding the detection limit issue of the aqua regia data set), and Co with increasing Co/Ni, whereas there is no trend for other ore metals such as Zn, or non-ore associated elements that may be of hydrothermal origin in VMS systems, such as Ba (Fig. 6).

Trace metals and metalloids in Windy Craggy sulfide minerals

The LA-ICP-MS mapping for this study was focused on deriving trace-element compositions of sulfide minerals, as opposed to detailed mapping to determine zonation or distribution within sulfide grains (e.g. Mathieu, 2019; Table 1). The greenschist-grade metamorphism of the Windy Craggy deposit and host rocks may have potentially modified the original element distributions of the sulfide minerals in the mineralization (Peter et al., 2014), so the aim was to determine the occurrence and abundance of key metals and metalloids that might indicate a magmatic contribution of metals to the mineralizing hydrothermal system, as suggested by fluid inclusion LA-ICP-MS results (Schmidt et al., 2019). Sulfide mineral LA-ICP-MS analyses have been subdivided on the basis of location within the deposit (massive sulfide, stringer zone, exhalite, gold zone) and rock type (mafic volcanic flows, mafic tuff, argillite) with further subdivision based on sulfide mineral (pyrite, chalcopyrite, pyrrhotite; Fig. 7, 8).

Variation of selected metals are shown relative to variation in Co/Ni values. Zinc, manganese, gallium, barium, and chromium generally decrease as Co/Ni values increase (Fig. 7a–e). Sulfide minerals in the massive-sulfide and gold zone have the highest Co/Ni values, generally greater than 100 (except for two samples from the gold zone). In contrast, sulfide minerals in the mafic volcanic flows, mafic tuff, and argillite have generally low Co/Ni values: less than 10, with most less than 1. Conversely, Bi, Mo, Te, Au, As, and Sb generally have the highest concentrations in sulfide minerals in samples from the massive sulfide, gold zone, and some stockwork (Fig. 8a–f). Significantly, sulfide-mineral trace-element chemistry is controlled by location within the deposit, rather than showing any significant preferences for specific sulfide minerals (Fig. 7, 8). For example, Co has abundances greater than 500 ppm in pyrite, chalcopyrite, and pyrrhotite.

DISCUSSION

Origin of Co enrichment in the Windy Craggy deposit

Windy Craggy is an atypical VMS deposit compared to many ancient VMS and modern seafloor massive-sulfide (SMS) deposits in that it is rich in Cu (relative to Pb and Zn), with generally low Zn abundances (Fig. 6a, 9). Compared to global and Canadian VMS deposits, Windy Craggy is dominantly rich in Cu, with most of the 3500 Geddes geochemical data having Cu-Zn greater than 1 (Fig. 9). Furthermore, Cu-Zn values are not log-normally distributed, but are heavily skewed to high Cu-Zn values (Fig. 9b). On the modern seafloor, only ultramafic, rock-hosted deposits have average Cu greater than Zn. Windy Craggy is rich in Co, but with only minor (relatively insignificant), discrete Co sulfide minerals such as cobaltite (Peter and Scott, 1999). The main deposit types that provide most global production for Co include sediment-hosted Cu-Co deposits, Ni-Co laterite deposits, and magmatic Ni-Cu (-Co–platinum-group element) sulfide deposits (Slack et al., 2017).

Until recently, the Co-rich nature of the Windy Craggy deposit was enigmatic. The possible Co sources include direct contributions of magmatic metals (e.g. Peter, 1992), leaching of footwall mafic volcanic rocks and/or argillic sedimentary rocks (e.g. Jowitt et al., 2012), or enhanced Co mobility in hydrothermal fluids with a magmatic component (e.g. Brugger et al., 2016) or a high-salinity hydrothermal fluid (e.g. Peter and Scott, 1999; Schmidt et al., 2018, 2019). We will consider each alternative in light of the findings of this current study.

One possible source of Co is leaching from the footwall mafic volcanic rocks and/or the argillite. Jowitt et al (2012) investigated alteration and metal redistribution in the Troodos ophiolite in Cyprus and suggested that Co, unlike Zn, Mn, Ni, and Cu, was not leached from the rocks, but was only redistributed within the sheeted dyke complex. The implication of their results is that Co/Ni values of the alteration zone (zone of leaching) would increase and, presumably, Co/Ni values would be lower where metals are subsequently deposited. If these results from Troodos are applicable to Windy

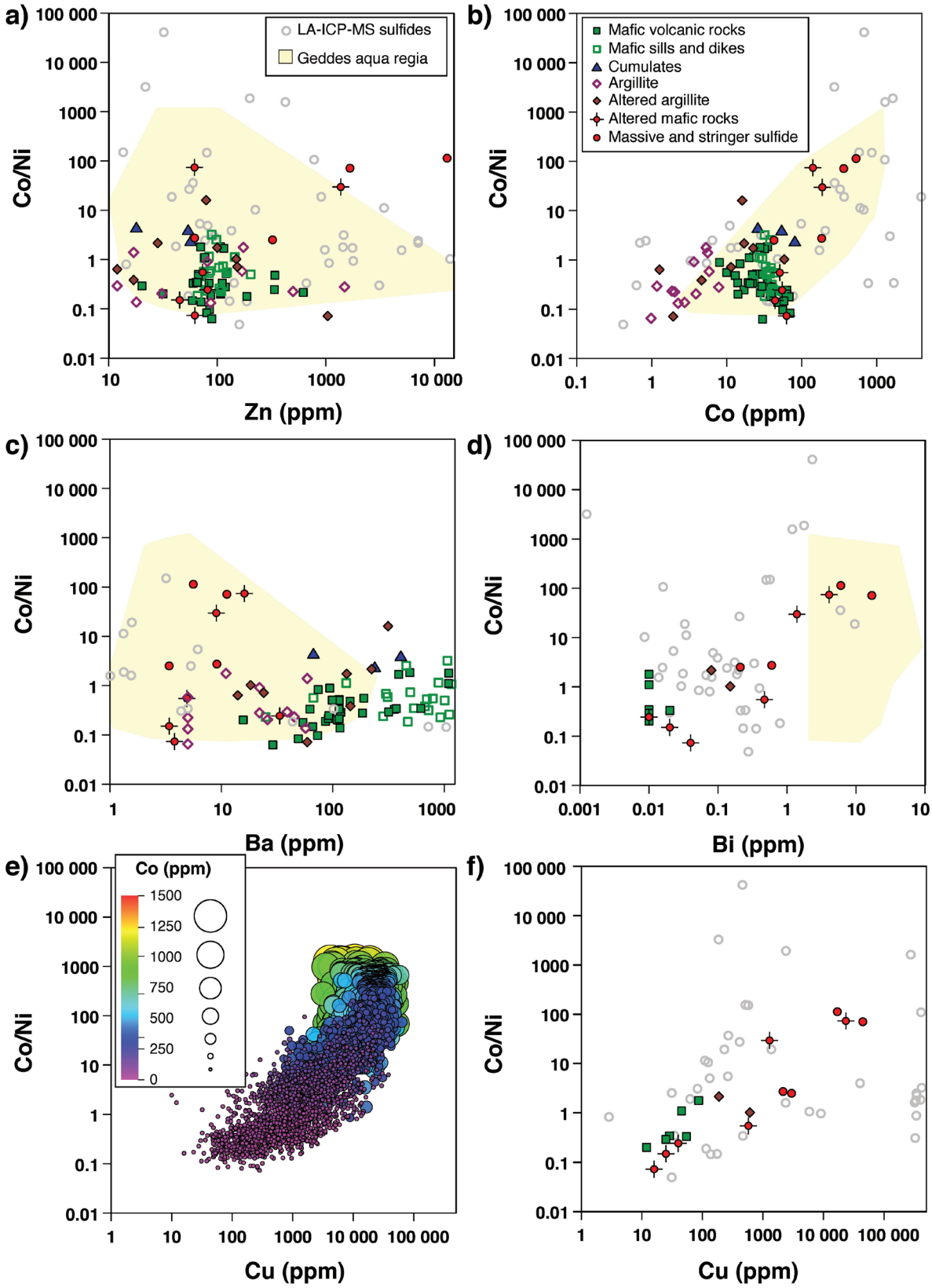

Figure 6. Plots of whole-rock geochemical data from the Windy Craggy deposit, northwestern British Columbia showing the relationship between Co/Ni value and **a)** Zn, **b)** Co, **c)** Ba, **d)** Bi, and **e**, **f**) Cu for various rock types. Also shown are the results of laser-ablation inductively coupled plasma mass spectrometry (LA-ICP-MS) analyses of all sulfide minerals sampled in this study and, in a–d, fields showing the aqua regia geochemical data (*after* Geddes Resources Ltd., unpub. rept., 1990). In e), proportional circles and colour ramp based on Co abundances are shown.

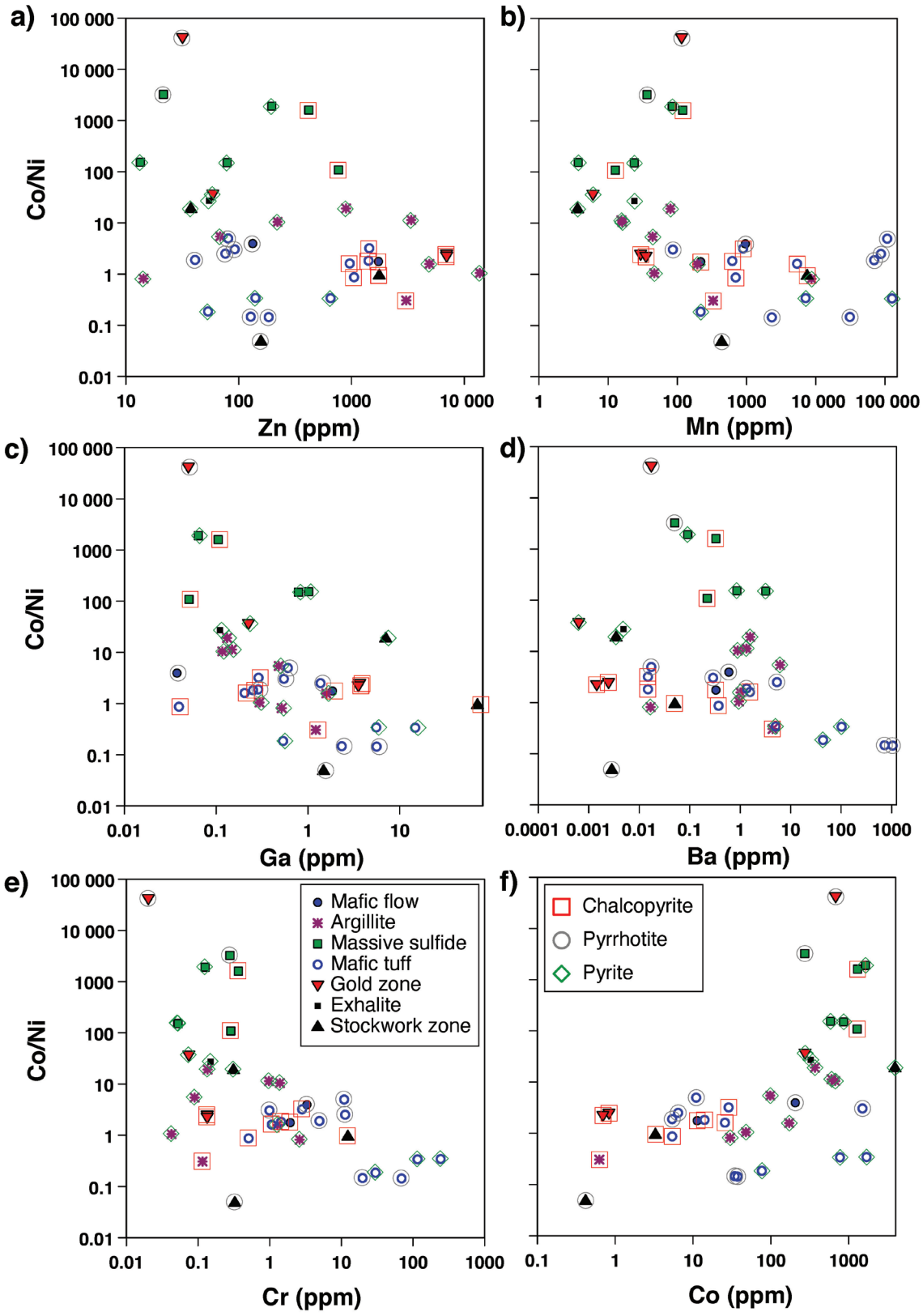

Figure 7. Plots of laser-ablation inductively coupled plasma mass spectrometry (LA-ICP-MS) data from sulfide minerals from the Windy Craggy deposit, northwestern British Columbia generated using iolite and Monocle (Petrus et al., 2017), showing the relationship between Co/Ni value and **a)** Zn, **b)** Mn, **c)** Ga, **d)** Ba, **e)** Cr, and **f)** Co.

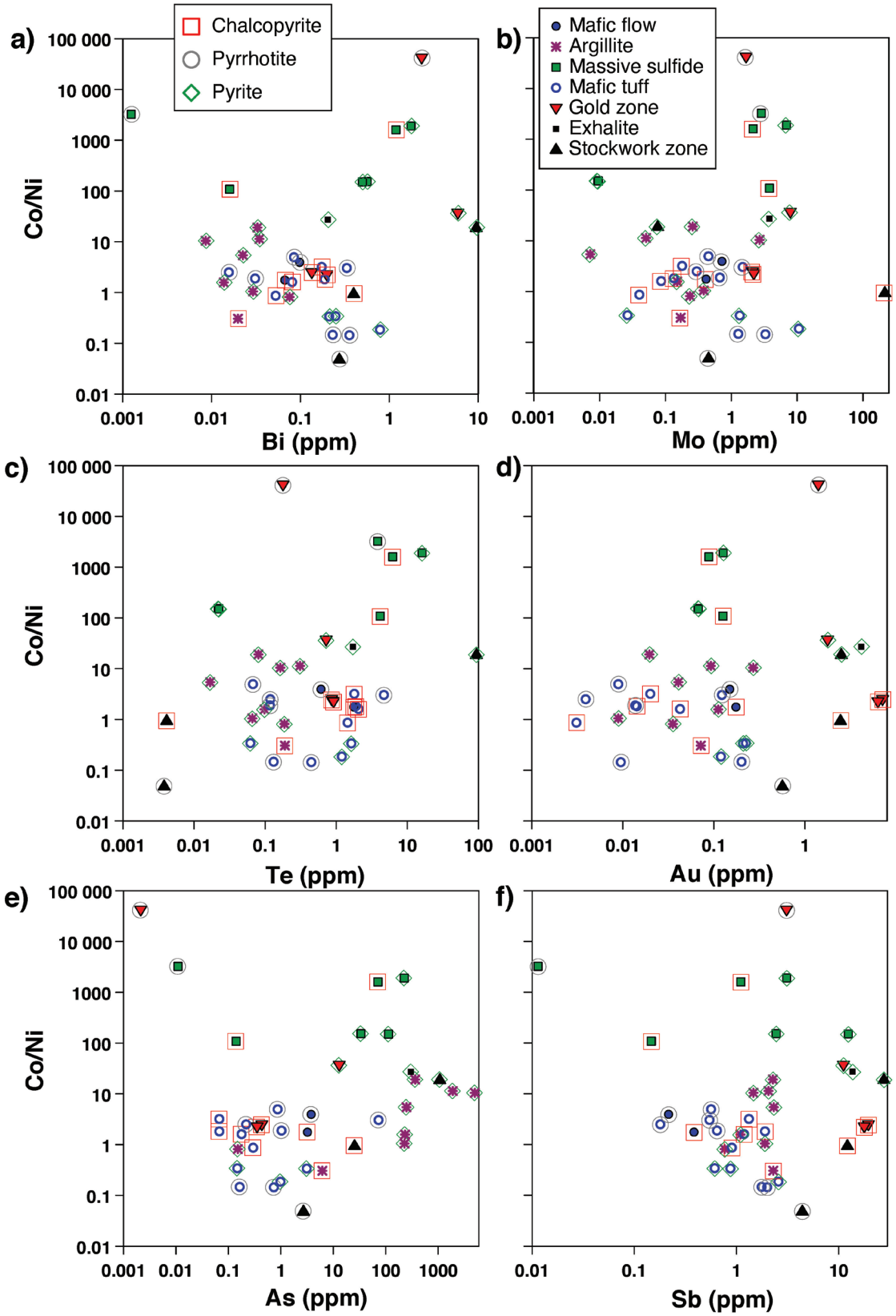

Figure 8. Plots of laser-ablation inductively coupled plasma mass spectrometry (LA-ICP-MS) data from sulfide minerals from the Windy Craggy deposit, northwestern British Columbia, generated using iolite and Monocle (Petrus et al., 2017), showing the relationship between Co/Ni value and **a)** Bi, **b)** Mo, **c)** Te, **d)** Au, **e)** As, and **f)** Sb.

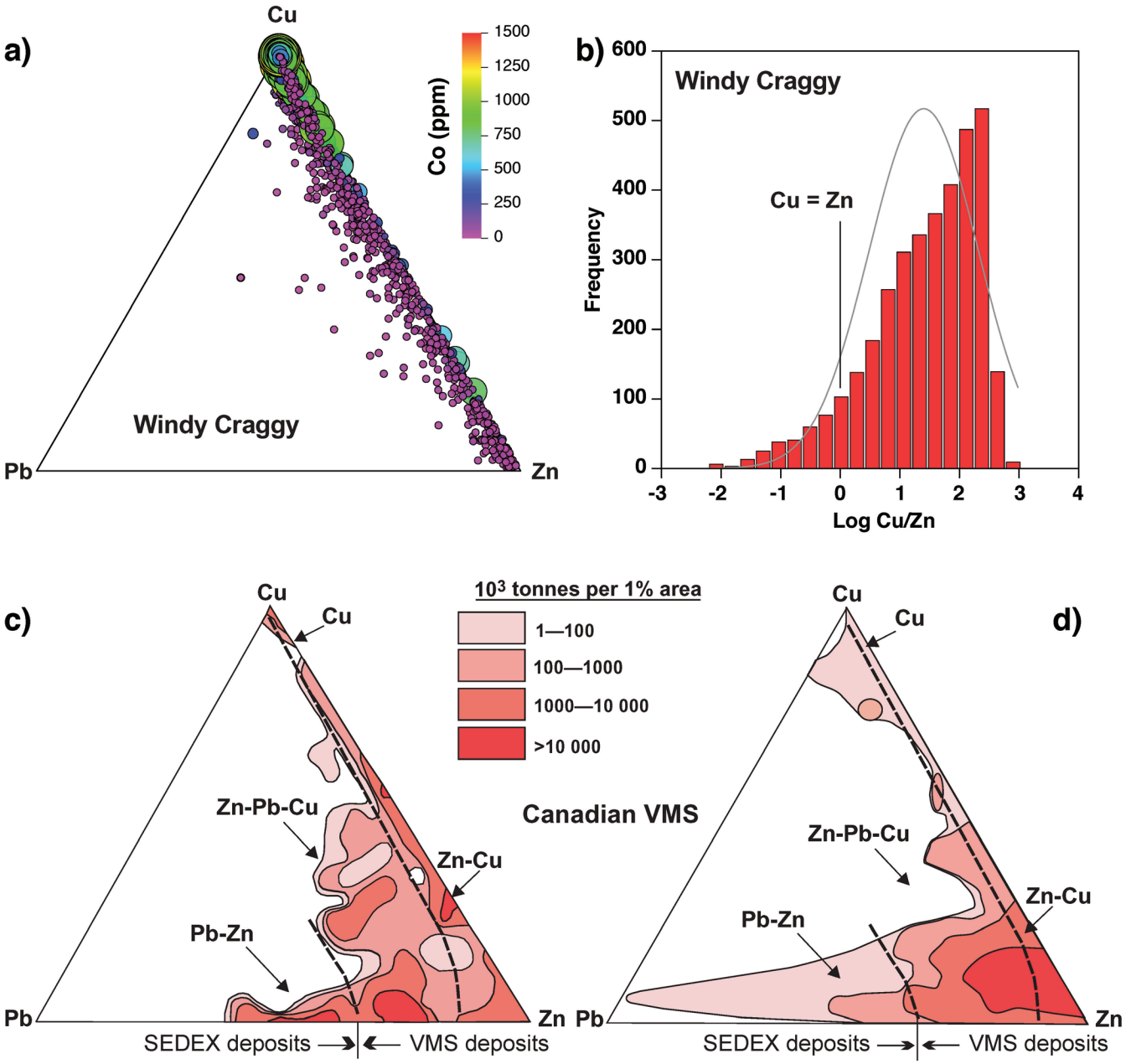

Figure 9. a) Ternary Cu-Zn-Pb plot for the approximately 3500 Geddes aqua regia data points collected at the Windy Craggy deposit, northwestern British Columbia (Geddes Resources Ltd, unpub. rept., 1990), with data points coloured and proportionally sized based on Co content; **b)** histogram of Cu-Zn values for the Geddes aqua regia data from Windy Craggy. Note that the vast majority of samples (3214 of 3521) have Cu greater than Zn; **c**, **d)** ternary Cu-Zn-Pb plots for c) global and d) Canadian volcanogenic massive-sulfide deposits for comparison (*modified from* Galley et al., 2007).

Craggy, hydrothermal leaching of the footwall rocks at Windy Craggy would have been unlikely, given that as Cu (and Fe) increases in the aqua regia assay data, Co/Ni values also increase (Fig. 6e), consistent with greater mobility of Co in the Windy Craggy ore-forming fluids compared to Ni (or Zn, Mn, and Cr). Thus, if leaching of Co from footwall rocks was a major control on the Co content of sulfide mineralization at Windy Craggy, this implies that Co was significantly more mobile in the hydrothermal fluids than other first row transition metals (i.e. Mn, Fe, Ni, and Cu). Note also that the Co contents of both altered and unaltered argillite samples are considerably lower than that of the mafic volcanic and intrusive rocks (Fig. 5d).

Brugger et al. (2016) reviewed metal speciation data and showed that, at typical hydrothermal fluid temperatures (up to only 300°C) and low to moderate salinities (a_{Cl} ~ –0.5 to 0), Co complexes to a greater extent as a tetrahedral Cl complex than does Ni, which forms octahedral complexes. These octahedral complexes are less soluble, accounting for

the higher Co/Ni in hydrothermal fluids of salinities typical of modern SMS hydrothermal systems. The consistently higher Co/Ni values in the sulfide minerals and more hydrothermally altered host rocks and mineralization at Windy Craggy are consistent with a greater mobility of Co in the magmatic-hydrothermal fluids that formed the deposit. In this context, we are referring to 'magmatic-hydrothermal' as a hydrothermal fluid in a VMS system, with appreciable magmatic volatile (which may or may not include metals) concentrations (e.g. de Ronde et al., 2005; Leybourne et al., 2012b). An alternative explanation was suggested by Nadeau et al. (2010) for porphyry copper deposits, in which they postulated that metal-rich sulfide melts are produced by the degassing of magmas. These metals could then be added to a hydrothermal fluid by the leaching of sulfide globules; the globules have elevated, but co-equal, proportions of Ni and Co (Nadeau et al., 2010). Similarly, Hunter et al. (2020) found Cu, Co, Sn, and Ag deposited as alloys on the surfaces of vesicles from a variety of mafic volcanoes, and suggested these were produced by a magmatic volatile phase; however, to explain the elevated Co/Ni values observed at Windy Craggy and other magmatic-hydrothermal deposits (including VMS and porphyry deposit types) would require either that Ni is less mobile in the fluids, or that Ni is subsequently lost to another sulfide phase (e.g. FeNiS and smythite [$(Fe,Ni)_9S_{11}$] were observed in the samples studied by Nadeau et al. (2010)).

The salinities of fluid inclusions in quartz from the Windy Craggy deposit, assuming they contain samples of the mineralizing fluids, are generally higher than typical of VMS systems (e.g. an average of 9.3 weight per cent equivalent NaCl at Windy Craggy versus 3.2 weight per cent equivalent NaCl at a typical VMS; Peter and Scott, 1999; Schmidt et al., 2018). There are many ways to increase the salinity of hydrothermal fluids, such as magma degassing, leaching of Cl-enriched phases in the crystallized rock, seawater alteration of footwall rocks, and phase separation, with Cl enriched in the residual fluid phase (Webster et al., 2018). The higher salinities of fluids at Windy Craggy may have enhanced the solubility and transport of Co compared to other VMS deposits. The elevated salinities of Windy Craggy fluids can be explained by a higher proportion of saline magmatic fluids (brines). Although we cannot rule out a role for phase separation to enhance salinity, we have no good evidence for phase separation because fluid inclusions at Windy Craggy are dominantly two phases (liquid-vapour) and no daughter crystals have been observed; phase separation may have occurred elsewhere in the system (Peter and Scott, 1999; Schmidt et al., 2018). Cobalt is less volatile than metals/metalloids such as As, Sb, Mo, Te, and Bi (Rubin, 1997); therefore, if Co is directly added from degassing magmas to the magmatic-hydrothermal fluids at Windy Craggy along with more volatile elements, as shown here (Fig. 8 shows the samples with the highest Bi, Te, Sb, and Mo have elevated Co/Ni values) and in fluid inclusions (Schmidt et al., 2019), this implies that the dominant addition was via a saline fluid as opposed to a volatile phase. This does not mean there was no devolatilization of a Windy Craggy magma chamber, just that there is no requirement for addition of metals via that mechanism. Chloride is soluble in mafic melts, in particular in alkalic rocks, at weight per cent concentrations, making Cl-rich volatile phases unlikely (Webster et al., 2018). Mixing of magmatic fluids with modified seawater (brines) has also been invoked to explain the high Co contents and presence of cobaltite in the sediment-hosted (but likely of magmatic-hydrothermal origin) Cu-Co deposits in the Idaho cobalt belt, U.S.A. (Saintilan et al., 2017). Cobalt enrichment is present in porphyry copper deposits due to its increased solubility in high-temperature fluids (Huston et al., 1995).

The mafic composition of the igneous rocks at Windy Craggy likely provides another fundamental control on Co contents. In mafic rocks, olivine is the major host for Co in the early fractionating phases (Ehlers et al., 1992; Beattie, 1994). Although not all VMS deposits with elevated Co contents are characterized by ultramafic host rocks, SMS deposits that are actively forming off-axis of the Mid-Atlantic Ridge with ultramafic rocks in their footwalls are commonly cobaltiferous (e.g. TAG deposit; Grant et al., 2018), as is also the case for Co-rich VMS deposits in the Ural Mountains (Nimis et al., 2008). Nickel also preferentially partitions into olivine (e.g. Ehlers et al., 1992; Li and Ripley, 2010), so that the breakdown of olivine (if it is the primary source of Co) during hydrothermal alteration implies greater mobility of Co compared to Ni, as discussed above. The deeper footwall is inaccessible due to structural dismemberment and lack of exposure so we have no record of ultramafic rocks at Windy Craggy, but many of the flows have elevated MgO (>10 weight per cent).

Cobalt distribution within pyrite grains is typically heterogeneous because it tends to follow growth zoning (e.g. porphyry copper deposits; Mathieu, 2019). The distribution of Co within pyrite grains can be modified by subsequent metamorphism. As metamorphic grade increases, the Co will migrate within the grain and form a Co-rich rim near the grain border (Craig et al., 1998). The highest Co abundances at Windy Craggy occur in the three regions (stockwork zones, massive sulfide, and gold zone) that would have formed from relatively high-temperature fluids (i.e. approximately 300–350°C; Fig. 6). Zinc decreases with increasing Co/Ni (Fig. 6a), consistent with the generally low Zn contents in the Windy Craggy deposit (Peter, 1992). Zinc is typically deposited in the lower temperature portions of VMS systems (e.g. Ohmoto, 1996), so the inverse relationship between Co/Ni and Zn may reflect either less Zn in the system, despite the presence of abundant Zn in seafloor mafic volcanic rocks (Doe, 1994), or that Zn-rich parts of the Windy Craggy deposit were never formed (i.e. Zn was lost to seawater because of high temperature) or not preserved (i.e. zone-refined out of the system; Ohmoto, 1996). One Zn-rich part of the deposit, located in the north orebody, contains up to 5 weight per cent Zn (Peter, 1992); this may represent overprinting by lower temperature fluids during the waning of the Windy Craggy ore-forming event(s).

Finally, the Windy Craggy deposit has significant pyrrhotite as a primary phase (*see* Fig. 3; Peter, 1992; Peter and Scott, 1999). Although pyrrhotite is common in modern SMS sulfide hydrothermal-vent deposits on mid-ocean ridges, especially those influenced by sediment accumulation such as Middle Valley, Juan de Fuca Ridge (Leybourne and Goodfellow, 1994), Guaymas Basin, Gulf of California (Peter and Scott, 1988), or Loki's Castle, Mid-Atlantic Ridge (Pedersen et al., 2010), it is rare in SMS deposits in arc and back-arc settings (Windy Craggy is interpreted to have formed via a slab-window in a back arc; Peter et al., 2014), owing to the generally more oxidizing conditions of the mantle source at arcs as a result of subduction zone processes (e.g. Kelley and Cottrell, 2012; Wysoczanski et al., 2012). Pyrrhotite is a common sulfide mineral in other Besshi-type deposits and sediment accumulation is also common (e.g. Crowe et al., 1992; Nimis et al., 2008). Alkalic rocks with known sulfide mineralization are rare in modern arc and back-arc settings, although recent studies at Nifonea volcano in the Vate Trough, New Hebrides, have shown that the sulfide chimneys are rich in pyrrhotite (Anderson et al., 2016) and vent fluids are rich in Co (Schmidt et al., 2017); however, it is unclear how changes in the reduction-oxidation (redox) conditions at Besshi-type deposits would result in enhanced Co mobility; in low-temperature aqueous systems, Co shows a strong affinity for Mn, and is enriched in seafloor Mn nodules and crusts (e.g. Hein et al., 1988; Hein et al., 2008). Although some Besshi-type deposits have organic-rich shales in their footwall succession, this is not the case at Windy Craggy, where unaltered argillites in the footwall have organic-C contents of less than 2.5 weight per cent (average = 1.1 weight per cent; Peter, unpub. data, 1992). Thus, the redox control does not appear to be related to an interaction with reducing footwall sedimentary rock types, at least at Windy Craggy.

Magmatic contributions to the Windy Craggy deposit

One of the primary goals of this research was to investigate possible direct magmatic volatile contribution of metals to the Windy Craggy deposit. The extent to which there are direct contributions of metals by degassing from magma chambers to VMS deposits has been the subject of debate in the literature. Some studies have suggested, and have shown via mass-balance modelling, that most or all of the metals in VMS deposits, both in the ancient rock record and in modern SMS systems, can be explained by the leaching of metals from footwall rocks by acidic, reducing, hydrothermal fluids; this is the commonly accepted model for the formation of VMS deposits (e.g. Galley et al., 2007). For example, Jowitt et al. (2012) suggested that a 2 km^3 epidosite alteration zone with depleted metal contents (compared to unaltered protoliths) in the Troodos ophiolite, Cyprus, could account for the contained metals in the VMS deposits. Conversely, work on arc-related SMS systems, as well as some back-arc systems, has shown that there is excellent evidence for significant contributions of gases (e.g. CH_4, H_2S, ^3He, SO_2, CO_2) from magmatic volatiles from high-level magma chambers, and many of these studies have suggested that metals may also be contributed by degassing magmas, in addition to hydrothermal leaching (e.g. de Ronde, 1995; Yang and Scott, 1996, 2006; Huston et al., 2001; Beaudoin et al., 2007; Leybourne et al., 2012b; Timm et al., 2012; Wysoczanski et al., 2012; Hunter et al., 2020). Many back-arc systems show seawater-dominated systems with less evidence for magmatic gas inputs, for example, the Tinakula deposit, Solomon Islands (Anderson et al., 2019).

Although modern mid-ocean ridge SMS systems (which have been studied extensively and—by analogy—were the basis for earlier models of ancient VMS deposits) more commonly show less evidence for magmatic contributions, these settings are less likely to be representative of ancient VMS deposits because the ultimate fate of oceanic crust (and any SMS) is subduction. Thus, modern arc and back-arc systems are much more likely to represent modern analogues of ancient VMS deposits (Hannington et al., 2005). Although magmatic contributions are increasingly being recognized as likely in VMS systems, there is currently no consensus as to which metals are representative of this contribution. In a study of trace-element distribution in sulfide minerals from hydrothermal black smokers from the PACMANUS hydrothermal vent field near Papua New Guinea, Wohlgemuth-Ueberwasser et al. (2015) suggested that the presence of Pb, As, Sb, Bi, Hg, and Te in the sulfide precipitates is indicative of contribution of magmatic volatiles. Sulfur isotope compositions for sulfide minerals that extend to more negative values than typically found at mid-ocean ridges are commonly cited as evidence for magmatic volatile contributions, for example, $\delta^{34}S$ values as low as –7.4‰ at SuSu Knolls and PACMANUS (Reeves et al., 2011; Yeats et al., 2014); however, sulfur isotope values of sulfide minerals from Windy Craggy are typical of mid-ocean ridge and back-arc systems (most samples measure –0.5–3‰ $\delta^{34}S$, with two samples having more negative values, to –6‰; Peter and Scott, 1999; Anderson et al., 2019). Peter and Scott (1999) attributed the rare, more negative $\delta^{34}S$ values at Windy Craggy to biogenic sulfate reduction, although magmatic degassing and sulfur disproportionation cannot be ruled out.

Patten et al. (2019), in a study of modern SMS sulfide mineralization at Ocean Drilling Program site 786B in the Izu-Bonin fore arc, suggested that Se, S, and Au contents are in excess of what could be explained by hydrothermal leaching and Se/S values increase in the core of the alteration zone; based on these characteristics, they concluded that these elements were likely derived from magmatic degassing. At Windy Craggy, Se/S values generally decrease with increasing Sb, As, Te, Bi, and Cu (not shown). Other studies have instead suggested that Te and Bi are most indicative of a direct magmatic contribution, for example, in active back-arc systems (Wohlgemuth-Ueberwasser et al., 2015). Thus,

there is evidence in the LA-ICP-MS sulfide data that there was likely a magmatic component to the Windy Craggy mineralizing fluid (and the sulfide minerals precipitated from it); this is shown particularly by enrichments in Te, Bi, Au, and, to a lesser extent, Sb in the higher temperature parts of the Windy Craggy system (Fig. 8). Selenium does not show any systematic trends of enrichment in the Windy Craggy sulfide minerals. These results are consistent with the presence of elevated Bi and Sb compared to Cu in fluid inclusions at Windy Craggy (Schmidt et al., 2019).

Are some (most) metals derived directly from crystallizing magmas?

The aim of this and companion studies by Schmidt et al. (2018, 2019) was to determine if some of the metal/metalloid budget of the Windy Craggy deposit was contributed directly by fractionating magmas, as opposed to leaching of footwall rocks by (modified seawater) hydrothermal fluids, as suggested by classical VMS deposit models. There is an ongoing debate regarding the sources of metals and volatiles in VMS deposits and their modern, actively forming SMS analogues, ranging from all or most metals sourced through the leaching of footwall rocks by hydrothermal fluids to partial to complete contributions from degassing magmas beneath the site of hydrothermal venting/sulfide deposition (de Ronde, 1995; Peter and Scott, 1999; de Ronde et al., 2005; Huston et al., 2011; Leybourne et al., 2012b). There is also disagreement in the literature as to what constitutes good evidence for magmatic contributions (discussed in detail by Huston et al. (2011)).

Individual studies have proposed different element suites that are contributed directly from the magma: Patten et al. (2019; Se, S, and Au), Wohlgemuth-Ueberwasser et al. (2015; Pb, As, Sb, Bi, Hg, and Te), Martin et al. (2020; Se, Cu, and Au). Huston et al. (2011) suggested that, for VMS deposits, only those deposits that are rich in Cu and Au with significant aluminous alteration and reduced, Sn-rich deposits show evidence of significant contributions directly from degassing magmas. Even in magmatic-hydrothermal systems such as porphyry copper deposits, where there is general consensus that metals and S are added via direct magmatic contributions (e.g. Sillitoe, 2010; Richards, 2011), the pathway or mechanism by which this addition happens is not entirely clear. Possibilities include addition via degassing (e.g. Sillitoe, 2010; Richards, 2011), degassing of underplated mafic melts (Hunter et al., 2020), leaching of previously exsolved sulfide melts (e.g. Nadeau et al., 2010), and leaching of sedimentary rocks along the fluid flow pathways of the magmatic-hydrothermal systems that form porphyry copper deposits (e.g. Mathieu, 2019).

We have shown here, based on whole-rock data and LA-ICP-MS measurements of sulfide minerals, as well as previously with LA-ICP-MS measurements of fluid inclusions at Windy Craggy (Schmidt et al., 2019), that metals/metalloids such as Bi, Sn, Sb, and probably Mo, Tl, and Te, appear to have been enriched in the deposit relative to other ore-associated metals, such as Zn, and lithophile elements that are typically associated with alteration in and around VMS deposits (e.g. Ba). Although volatiles are clearly added by magma degassing in many VMS and SMS systems, there is a lack of consensus as to what constitutes a 'magmatic' metal (compared to one added by leaching), and there may be a degree of circularity to the entire debate. In VMS systems, most of the footwall rocks represent the products of prior injections of melts into the magma chamber. Thus, many (most to all?) metals that are enriched in the melt and that might be contributed directly from the fractionating magma are likely also enriched in the rocks that previously erupted/intruded to form the footwall to the VMS deposit.

Figure 10 presents samples from the Windy Craggy deposit and rocks from other settings, normalized to N-type mid-ocean ridge basalt (MORB) values. This figure demonstrates that, for many metals/metalloids commonly considered to be indicative of magmatic contributions in a variety of deposit types (e.g. As, Se, Mo, Ag, Sn, Sb, W, Tl, Bi, and Te), the unaltered (or least altered in the case of Windy Craggy) igneous rocks show positive anomalies compared to MORB for some of these metals compared to lithophile elements (Fig. 10a; Co, As, and Se are not enriched compared to MORB in the least altered rocks).

Figure 10. N-type mid-ocean ridge basalt (MORB)–normalized plots of selected elements: **a)** Windy Craggy deposit mafic rocks (least altered and altered) and sulfide-rich samples; **b)** laser-ablation inductively coupled plasma mass spectrometry (LA-ICP-MS) data from Windy Craggy deposit pyrite and pyrrhotite samples, subdivided into mafic rocks, argillites, and samples from massive sulfide and stringer zones; and, for comparison, **c)** mafic rocks from the West Rota system (Mariana Arc), with unaltered basalts and basalts with elevated loss on ignition (LOI) and S greater than 1 weight per cent (*after* Leybourne and Hein, work in progress, 2020); **d)** felsic rocks from the West Rota caldera (Mariana Arc), with least-altered felsic rocks (low LOI, S < 1.5 weight per cent) and highly hydrothermally altered felsic rocks with elevated LOI and S greater than 1.5 weight per cent (*after* Leybourne and Hein, work in progress, 2020); **e)** fresh basaltic rocks from Rumble II West caldera, Kermadec Arc (*after* Leybourne et al., 2012a; Timm et al., 2016) and LA-ICP-MS data of chalcopyrite and pyrite (*after* Leybourne and Layton-Matthews, work in progress, 2020); and **f)** fresh basaltic rocks from the West Valley segment, subdivided by N-type MORB and D-type MORB (*after* Leybourne et al., work in progress, 2020). Elements highlighted with vertical orange bars (As, Se, Mo, Ag, Sn, Sb, W, Tl, Bi, and Te) are commonly considered as evidence of magmatic contributions (Co and Pb are also highlighted—see text). Normalizing values for N-type MORB *after* Gale et al. (2013), with additional values *after* Sun and McDonough (1989; Sb) and Leybourne et al. (work in progress, 2020); As, Ag, In, Re, and Bi). Gold and selenium set to 0.01 and 1 ppm, respectively.

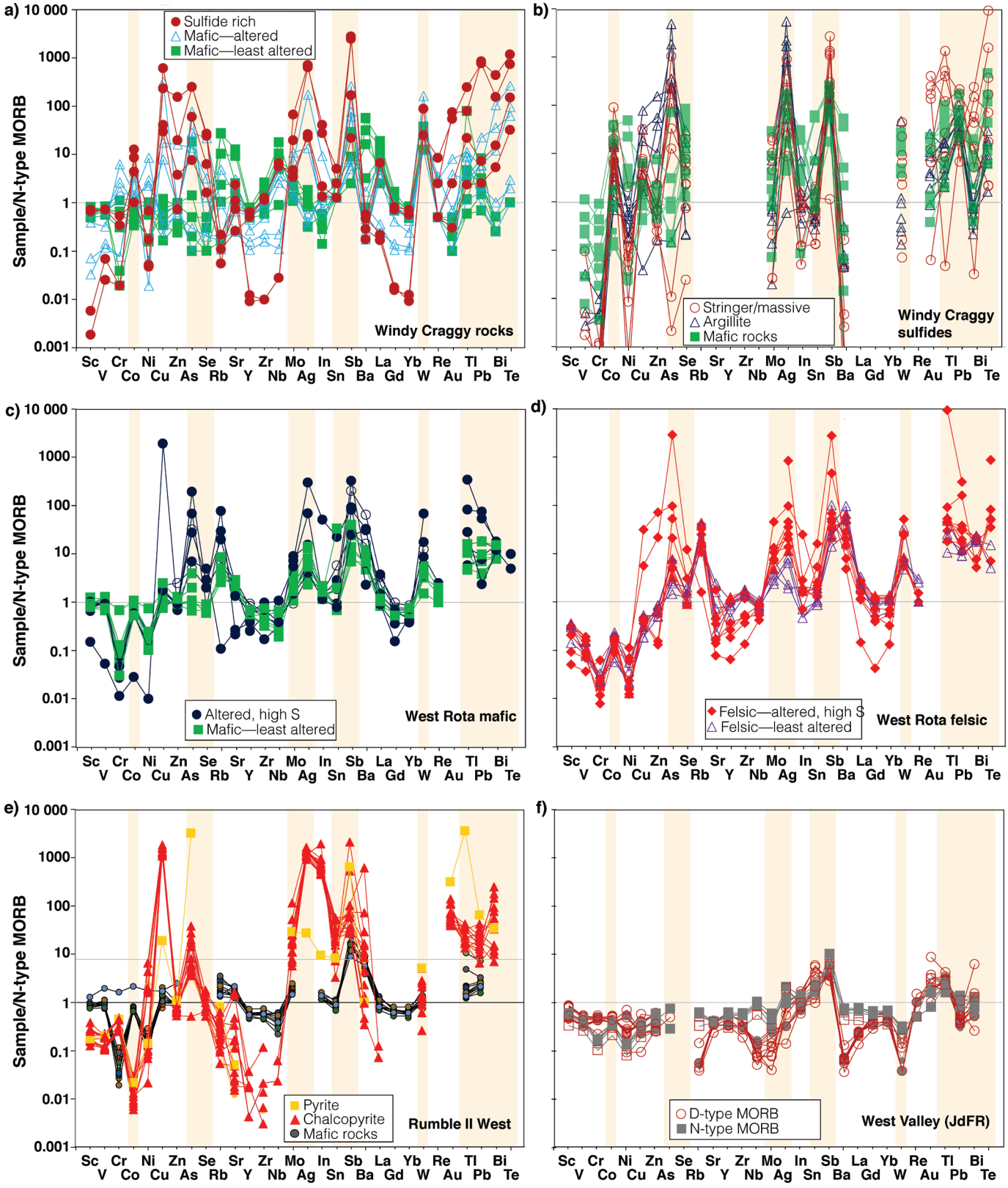
a)
Sulfide rich
Mafic—altered
Mafic—least altered
Windy Craggy rocks
b)
Stringer/massive
Argillite
Mafic rocks
Windy Craggy sulfides
c)
Altered, high S
Mafic—least altered
West Rota mafic
d)
Felsic—altered, high S
Felsic—least altered
West Rota felsic
e)
Pyrite
Chalcopyrite
Mafic rocks
Rumble II West
f)
D-type MORB
N-type MORB
West Valley (JdFR)
Sample/N-type MORB
10 000
1000
100
10
1
0.1
0.01
0.001
Sc V Cr Co Ni Cu Zn As Se Rb Sr Y Zr Nb Mo Ag In Sn Sb Ba La Gd Yb W Re Au Tl Pb Bi Te

These anomalies are enhanced as a result of hydrothermal alteration (altered mafic rocks) and within the massive-sulfide portions of the deposit (Fig. 10a). Pyrite and pyrrhotite from Windy Craggy show similar anomalies, with the extent of the anomaly increasing toward the high-temperature (stringer and massive sulfide) core of the deposit relative to the lower temperature peripheries (sulfide minerals in the mafic rocks and argillites; Fig. 10b).

Rocks recovered from in and around West Rota caldera on the Mariana Arc show similar relationships (Fig. 10c, d). West Rota is characterized by small satellite cones dominated by fresh mafic volcanic rocks (Fig. 10c), whereas most rocks recovered from within the caldera are intermediate to felsic and range to highly altered with significant pyrite ± chalcopyrite (Fig. 10d; Leybourne and Hein, work in progress, (2020)). It has previously been observed that rocks recovered from Rumble II West caldera on the Kermadec Arc are anomalous in Pb, Sb, Mo, and Tl (Leybourne et al., 2012a); here, fresh mafic rocks are shown to also be anomalous in other so-called magmatic metals (Fig. 10e). Laser-ablation ICP-MS analyses of sulfide minerals from a black-smoker chimney fragment from Rumble II West show similar, enhanced, anomalies as the rocks from Rumble II West (Fig. 10e; Leybourne and Layton-Matthews, work in progress, 2020). Rocks in arcs are anomalous in many of these metals compared to mid-ocean ridge basalt, and porphyry copper deposits are common in arcs because metals are added to the mantle wedge by subduction-zone fluids and the resulting increase in the oxidation state of arc mantle compared to MORB mantle (Cooke et al., 2014). Figure 10f shows LA-ICP-MS results for fresh glass from the West Valley segment of the Juan de Fuca Ridge, indicating that the mantle from which the MORB is sourced is generally not enriched in most metals and metalloids considered to indicate magmatic contributions.

Thus, we suggest that the means by which various studies have tried answer the question of whether there are magmatic contributions or whether the metal budget of VMS deposits can result from hydrothermal leaching are not valid because the source rocks appear to be enriched in the 'magmatic volatile metals' and thus the enrichment of magmatic volatile metals in a sulfide deposit may simply be due to enriched source rock, not direct injection of magmatic fluid. Although there is evidence for elevated metal contents in melt inclusions (Yang and Scott, 1996; 2006), fluid inclusions (Schmidt et al., 2019), and sulfide globules in porphyry copper systems (Nadeau et al., 2010) that would suggest direct magmatic contributions, and Cu-Co-Sn-Ag alloys deposited on vesicle walls (Hunter et al., 2020), such metal enrichments can also result from the hydrothermal fluid leaching of metals from footwall and/or flanking volcanic rocks and intrusive equivalents. There is excellent evidence for the direct contribution of volatile gases (e.g. CH_4, SO_2, H_2S, ^3He, and CO_2) from degassing magmas in SMS systems (de Ronde et al., 2005, 2011; Reeves et al., 2011; Yeats et al., 2014), resulting in particularly acidic hydrothermal fluids; the extreme acidity that results in enhanced leaching of metals, including those generally considered immobile (Leybourne et al., 2012b).

CONCLUSIONS

In this paper, we present a LA-ICP-MS element composition study of pyrite, pyrrhotite, and chalcopyrite grains from different mineralization styles (stockwork/feeder zone, massive sulfide, and gold zone) at the Windy Craggy Cu-Co-Zn VMS deposit. These data are considered together with previously presented LA-ICP-MS data for fluid inclusion, and several thousand legacy bulk-rock geochemical analyses. The highest Au, Ga, Sn, V, W, As, Bi, Hg, In, Sb, Se, Te, Tl, Ag, Co, and Mo contents in these bulk samples occur within the gold zone at the northwest edge of the South sulfide body and/or stockwork zone from the South sulfide body. These elements are either below detection or present in very low abundances (<1 ppm) in the host rocks. These trends in sulfide chemistry are consistent with their direct magmatic contribution to the Windy Craggy deposit. Correlation of Co with these so-called 'magmatic elements' indicates that it too is of magmatic origin, perhaps sourced via fluids exsolved from a crystallizing mafic magma chamber; however, evidence from the composition of rocks and sulfide minerals from Windy Craggy and other modern SMS systems suggests that there is probably no meaningful distinction between hydrothermal leaching and direct magmatic contributions, based on metal budget considerations. We suggest that fluids that form VMS deposits are produced by 'magmatic-hydrothermal' fluids, whether metals are derived by the leaching of the igneous rocks or (partly) contributed by metal-bearing volatiles from their precursor magma.

ACKNOWLEDGMENTS

The LA-ICP-MS analysis portion of this study was completed as part of an M.Sc. thesis in conjunction with NRCan's Targeted Geoscience Initiative program. Funding was provided through the Volcanic and Sedimentary-hosted Base Metal Mineralization project's Activity VS-2.4: Fingerprinting fluid source regions and pathways of volcanogenic massive-sulfide deposits. Laboratory work was also supported by funding to the first author by the McDonald Institute, through the Canada First Research Excellence Fund. We thank John Jamieson and Melissa Anderson for thorough and constructively critical reviews that greatly improved the manuscript.

REFERENCES

Anderson, M.O., Hannington, M.D., Haase, K., Schwarz-Schampera, U., Augustin, N., McConachy, T.F., and Allen, K., 2016. Tectonic focusing of voluminous basaltic eruptions in magma-deficient backarc rifts; Earth and Planetary Science Letters, v. 440, p. 43–55. https://doi.org/10.1016/j.epsl.2016.02.002

Anderson, M.O., Hannington, M.D., McConachy, T.F., Jamieson, J.W., Anders, M., Wienkenjohann, H., Strauss, H., Hansteen, T., and Petersen, S., 2019. Mineralization and alteration of a modern seafloor massive sulfide deposit hosted in mafic volcaniclastic rocks: Economic Geology, v. 114, p. 857–896. https://doi.org/10.5382/econgeo.4666

Bajwah, Z.U., Seccombe, P.K., and Offler, R., 1987. Trace element distribution, Co: Ni ratios and genesis of the big cadia iron-copper deposit, New South Wales, Australia, January 1987, Mineralium Deposita, v. 22, no. 4, p. 292–300. https://doi.org/10.1007/BF00204522

Beattie, P., 1994. Systematics and energetics of trace-element partitioning between olivine and silicate melts: implications for the nature of mineral melt partitioning; Chemical Geology, v. 117, p. 57–71. https://doi.org/10.1016/0009-2541(94)90121-X

Beaudoin, Y., Scott, S.D., Gorton, M.P., Zajacz, Z., and Halter, W., 2007. Pb and other ore metals in modern seafloor tectonic environments; evidence from melt inclusions; Marine Geology, v. 242, no. 4, p. 271–289. https://doi.org/10.1016/j.margeo.2007.04.004

Bralia, A., Sabatini, G., and Troja, F., 1979. A revaluation of the Co/Ni ratio in pyrite as a geochemical tool in ore genesis problems; Mineralium Deposita, v. 14, p. 353–374. https://doi.org/10.1007/BF00206365

Brugger, J., Liu, W., Etschmann, B., Mei, Y., Sherman, D.M., and Testemale, D., 2016. A review of the coordination chemistry of hydrothermal systems, or do coordination changes make ore deposits?; Chemical Geology, v. 447, p. 219–253. https://doi.org/10.1016/j.chemgeo.2016.10.021

Butler, I.B. and Nesbitt, R.W., 1999. Trace element distributions in the chalcopyrite wall of a black smoker chimney: insights from laser ablation inductively coupled plasma mass spectrometry (LA–ICP–MS); Earth and Planetary Science Letters, v. 167, no. 3–4, p. 335–345. https://doi.org/10.1016/S0012-821X(99)00038-2

Campbell, R.B. and Dodds, C.J., 1979. Operation Saint Elias, British Columbia; in Current Research, Part A; Geological Survey of Canada, Paper 79-1A, p. 17–20. https://doi.org/10.4095/104819

Campbell, R.B. and Dodds, C.J., 1983. Geology of Tatshenshini River map area (114P), British Columbia; Geological Survey of Canada, Open File 926, 2 sheets. https://doi.org/10.4095/129621

Church, S.E., Mosier, E.L., and Motooka, J.M., 1987. Mineralogical basis for the interpretation of multi-element (ICP-AES), oxalic acid, and aqua regia partial digestions of stream sediments for reconnaissance exploration geochemistry; Journal of Geochemical Exploration, v. 29, p. 207–233. https://doi.org/10.1016/0375-6742(87)90078-1

Coney, P.J., Jones, D.L., and Monger, J.W.H., 1980. Cordilleran suspect terranes; Nature, v. 288, p. 329–333. https://doi.org/10.1038/288329a0

Cooke, D.R., Hollings, P., Wilkinson, J.J., and Tosdal, R., 2014. Geochemistry of porphyry deposits; Chapter 14 *in* Volume 13: Geochemistry of mineral deposits, Treatise on geochemistry, 2nd edition, (ed.) S.D. Scott; Elsevier, Oxford, UK, p. 357–381. https://doi.org/10.1016/B978-0-08-095975-7.01116-5

Craig, J.R., Vokes, F.M., and Solberg, T.N., 1998. Pyrite: physical and chemical textures; Mineralium Deposita, v. 34, p. 82–101. https://doi.org/10.1007/s001260050187

Crowe, D.E., Nelson, S.W., Brown, P.E., Shanks, W.C., and Valley, J.W., 1992. Geology and geochemistry of volcanogenic massive sulfide deposits and related igneous rocks, Prince William Sound, south-central Alaska; Economic Geology, v. 87, no. 7, p. 1722–1746. https://doi.org/10.2113/gsecongeo.87.7.1722

de Ronde, C.E.J., 1995. Fluid chemistry and isotopic characteristics of seafloor hydrothermal system and associated VMS deposits: potential for magmatic contributions; Mineralogical Association of Canada, Short Course Handbook 23, p. 479–509.

de Ronde, C.E.J., Hannington, M.D., Stoffers, P., Wright, I.C., Ditchburn, R.G., Reyes, A.G., Baker, E.T., Massoth, G.J., Lupton, J.E., Walker, S.L., Greene, R.R., Soong, C.W.R., Ishibashi, J., Lebon, G.T., Bray, C.J., and Resing, J.A., 2005. Evolution of a submarine magmatic-hydrothermal system: Brothers volcano, southern Kermadec arc, New Zealand; Economic Geology, v. 100, p. 1097–1133. https://doi.org/10.2113/gsecongeo.100.6.1097

de Ronde, C.E.J., Massoth, G.J., Butterfield, D.A., Christenson, B.W., Ishibashi, J., Ditchburn, R.G., Hannington, M.D., Brathwaite, R.L., Lupton, J.E., Kamenetsky, V.S., Graham, I.J., Zellmer, G.F., Dziak, R.P., Embley, R.W., Dekov, V.M., Munnik, F., Lahr, J., Evans, L.J., and Takai, K., 2011. Submarine hydrothermal activity and gold-rich mineralization at Brothers Volcano, Kermadec arc, New Zealand; Mineralium Deposita, v. 46, p. 541–584. https://doi.org/10.1007/s00126-011-0345-8

Deditius, A.P. and Reich, M., 2016. Constraints on the solid solubility of Hg, Tl, and Cd in arsenian pyrite; American Mineralogist, v. 101, p. 1451–1459. https://doi.org/10.2138/am-2016-5603

Deditius, A.P., Utsunomiya, S., Reich, M., Kesler, S.E., Ewing, R.C., Hough, R., and Walshe, J., 2011. Trace metal nanoparticles in pyrite; Ore Geology Reviews, v. 42, no. 1, p. 32–46. https://doi.org/10.1016/j.oregeorev.2011.03.003

Doe, B.R., 1994. Zinc, copper, and lead in mid-ocean ridge basalts and the source rock control on Zn/Pb in ocean-ridge hydrothermal deposits; Geochimica et Cosmochimica Acta, v. 58, p. 2215–2223. https://doi.org/10.1016/0016-7037(94)90006-X

Downing, B.W., Webster, M.P., and Beckett, R.J., 1990. The Windy Craggy massive-sulphide deposit, northwestern British Columbia, Canada; *in* Mineral deposits of the northern Canadian Cordillera, Yukon – northeastern British Columbia [field trip 14], (ed.) J.G. Abbott and R.J. Turner; Geological Survey of Canada, Open File 2169, p. 25–30. https://doi.org/10.4095/132328

Ehlers, K., Grove, T.L., Sisson, T.W., Recca, S.I., and Zervas, D.A., 1992. The effect of oxygen fugacity on the partitioning of nickel and cobalt between olivine, silicate melt, and metal; Geochimica et Cosmochimica Acta, v. 56, p. 3733–3743. https://doi.org/10.1016/0016-7037(92)90166-G

Gale, A., Dalton, C.A., Langmuir, C.H., Su, Y., and Schilling, J.G., 2013. The mean composition of ocean ridge basalts; Geochemistry, Geophysics, Geosystems, v. 14, p. 489–518. https://doi.org/10.1029/2012GC004334

Galley, A., Hannington, M., and Jonasson, I., 2007. Volcanogenic massive sulfide deposits, *in* Mineral deposits of Canada: a synthesis of major deposit-types, district metallogeny, the evolution of geological provinces, and exploration methods, (ed.) W.D. Goodfellow; Geological Association of Canada, Mineral Deposits Division, Special Publication No. 5, p. 141–161.

Grant, H.L.J., Hannington, M.D., Petersen, S., Frische, M., and Fuchs, S.H., 2018. Constraints on the behavior of trace elements in the actively-forming TAG deposit, Mid-Atlantic Ridge, based on LA-ICP-MS analyses of pyrite; Chemical Geology, v. 498, p. 45–71. https://doi.org/10.1016/j.chemgeo.2018.08.019

Hannington, M.D., de Ronde, C.E.J., and Petersen, S., 2005. Sea-floor tectonics and submarine hydrothermal systems; *in* Economic Geology, 100th anniversary volume, 1905–2005, (ed.) J.W. Hedenquist, J.F.H. Thompson, R.J. Goldfarb, and J.P. Richards; Society of Economic Geologists, Littleton, Colorado, p. 111–141. https://doi.org/10.5382/AV100.06

Hein, J.R., Schwab, W.C., and Davis, A.S., 1988. Co and Pt-rich ferromanganese crusts and associated substrate rocks from the Marshall Islands; Marine Geology, v. 78, no. 3-4, p. 255–283. https://doi.org/10.1016/0025-3227(88)90113-2

Hein, J.R., Schulz, M.S., Dunham, R.E., Stern, R.J., and Bloomer, S.H., 2008. Diffuse flow hydrothermal manganese mineralization along the active Mariana and southern Izu-Bonin arc system, western Pacific; Journal of Geophysical Research: Solid Earth, v. 113, no. B8. https://doi.org/10.1029/2007JB005432

Hunter, E.A.O., Hunter, J.R., Zajacz, Z., Keith, J.D., Hann, N.L., Christiansen, E.H., and Dorais, M.J., 2020. Vapor transport and deposition of Cu-Sn-Co-Ag alloys in vesicles in mafic volcanic rocks; Economic Geology, v. 115, no. 2, p. 279–301. https://doi.org/10.5382/econgeo.4702

Huston, D.L., Sie, S.H., Suter, G.F., Cooke, D.R., and Both, R.A., 1995. Trace elements in sulfide minerals from eastern Australian volcanic-hosted massive sulfide deposits; Part I, Proton microprobe analyses of pyrite, chalcopyrite, and sphalerite, and Part II, Selenium levels in pyrite; comparison with delta (super 34) S values and implications for the source of sulfur in volcanogenic hydrothermal systems; Economic Geology, v. 90, no. 5, p. 1167–1196. https://doi.org/10.2113/gsecongeo.90.5.1167

Huston, D.L., Brauhart, C.W., Drieberg, S.L., Davidson, G.J., and Groves, D.I., 2001. Metal leaching and inorganic sulfate reduction in volcanic-hosted massive sulfide mineral systems: Evidence from the paleo-Archean Panorama district, Western Australia; Geology, v. 29, p. 687–690. https://doi.org/10.1130/0091-7613(2001)029%3C0687:MLAISR%3E2.0.CO;2

Huston, D.L., Relvas, J.M.R.S., Gemmell, J.B., and Drieberg, S., 2011. The role of granites in volcanic-hosted massive sulphide ore-forming systems: an assessment of magmatic–hydrothermal contributions; Mineralium Deposita, v. 46, p. 473–507. https://link.springer.com/article/10.1007/s00126-010-0322-7

Itoh, S., 1976. Geochemical study of bedded cupriferous pyrite deposits in Japan; Bulletin of the Geological Survey of Japan, v. 27, no. 5, p. 245–377.

Jochum, K.P., Weis, U., Stoll, B., Kuzmin, D., Yang, Q., Raczek, I., Jacob, D.E., Stracke, A., Birbaum, K., Frick, D.A., Günther, D., and Enzweiler, J., 2011. Determination of reference values for NIST SRM 610-617 glasses following ISO guidelines; Geostandards and Geoanalytical Research, v. 35, p. 397–429. https://doi.org/10.1111/j.1751-908X.2011.00120.x

Jowitt, S.M., Jenkin, G.R.T., Coogan, L.A., and Naden, J., 2012. Quantifying the release of base metals from source rocks for volcanogenic massive sulfide deposits: effects of protolith composition and alteration mineralogy; Journal of Geochemical Exploration, v. 118, p. 47–59. https://doi.org/10.1016/j.gexplo.2012.04.005

Kase, K. and Yamamoto, M., 1988. Minerals and geochemical characteristics of ores from the Besshi-type deposits in the Sanbagawa belt, Japan; Mining Geology, v. 38, p. 203–214.

Keith, M., Haase, K.M., Klemd, R., Krumm, S., and Strauss, H., 2016. Systematic variations of trace element and sulfur isotope compositions in pyrite with stratigraphic depth in the Skouriotissa volcanic-hosted massive sulfide deposit, Troodos ophiolite, Cyprus; Chemical Geology, v. 423, p. 7–18. https://doi.org/10.1016/j.chemgeo.2015.12.012

Kelley, K.A. and Cottrell, E., 2012. The influence of magmatic differentiation on the oxidation state of Fe in a basaltic arc magma; Earth and Planetary Science Letters, v. 329–330, p. 109–121. https://doi.org/10.1016/j.epsl.2012.02.010

Large, R.R., Danyushevsky, L., Hollit, C., Maslennikov, V., Meffre, S., Gilbert, S., Bull, S., Scott, R., Emsbo, P., Thomas, H., Singh, B., and Foster, J., 2009. Gold and trace element zonation in pyrite using a laser imaging technique: implications for the timing of gold in orogenic and Carlin-style sediment-hosted deposits; Economic Geology, v. 104, p. 635–668. https://doi.org/10.2113/gsecongeo.104.5.635

Leybourne, M.I. and Goodfellow, W.D., 1994. Mineralogy and mineral chemistry of hydrothermally altered sediment, Middle Valley, Juan de Fuca Ridge; *in* Proceedings of the ocean drilling program, volume 139: scientific results, Middle Valley, Juan de Fuca Ridge, (ed.) M.J. Mottl, E.E. Davis, A.T. Fisher, and J.F. Slack; Texas A&M University, College Station, Texas, p. 155–206.

Leybourne, M.I., de Ronde, C.E.J., Wysoczanski, R.J., Walker, S.L., Timm, C., Gibson, H.L., Layton-Matthews, D., Baker, E.T., Clark, M.R., Tontini, F.C., Faure, K., Lupton, J.E., Fornari, D.J., Soule, S.A., and Massoth, G.J., 2012a. Geology, hydrothermal activity, and sea-floor massive sulfide mineralization at the Rumble II West mafic caldera; Economic Geology, v. 107, no. 8, p. 1649–1668. https://doi.org/10.2113/econgeo.107.8.1649

Leybourne, M.I., Schwarz-Schampara, U., de Ronde, C.E.J., Baker, E.T., Faure, K., Walker, S., Butterfield, D., Resing, J., Lupton, J., Hannington, M., Massoth, G., Clark, M., Timm, C., Graham, I., and Wright, I., 2012b. Submarine magmatic-hydrothermal systems at the Monowai volcanic centre, Kermadec Arc; Economic Geology, v. 107, no. 8, p. 1669–1694. https://doi.org/10.2113/econgeo.107.8.1669

Li, C. and Ripley, E.M., 2010. The relative effects of composition and temperature on olivine-liquid Ni partitioning: statistical deconvolution and implications for petrologic modeling; Chemical Geology, v. 275, no. 1–2, p. 99–104. https://doi.org/10.1016/j.chemgeo.2010.05.001

Loftus-Hills, G. and Solomon, M., 1967. Cobalt, nickel and selenium in sulphides as indicators of ore genesis; Mineralium Deposita, v. 2, p. 228–242. https://doi.org/10.1007/BF00201918

MacIntyre, D.G., 1984. Geology of the Alsek-Tatshenshini rivers area (114P); *in* Geological Fieldwork 1983; British Columbia Ministry of Energy, Mines and Petroleum Resources, British Columbia Geological Survey, Paper 1984-1, p. 173–184.

Martin, A.J., Keith, M., McDonald, I., Haase, K.M., McFall, K.A., Klemd, R., and MacLeod, C.J., 2019. Trace element systematics and ore-forming processes in mafic VMS deposits: Evidence from the Troodos ophiolite, Cyprus; Ore Geology Reviews, v. 106, p. 205–225. https://doi.org/10.1016/j.oregeorev.2019.01.024

Martin, A.J., Keith, M., Parvaz, D.B., McDonald, I., Boyce, A.J., McFall, K.A., Jenkin, G.R.T., Strauss, H., and MacLeod, C.J., 2020. Effects of magmatic volatile influx in mafic VMS hydrothermal systems: evidence from the Troodos ophiolite, Cyprus; Chemical Geology, v. 531, 119325. https://doi.org/10.1016/j.chemgeo.2019.119325

Mudd, G.M., Weng, Z., Jowitt, S.M., Turnbull, I.D., and Graedel, T.E., 2013. Quantifying the recoverable resources of by-product metals: the case of cobalt; Ore Geology Reviews, v. 55, p. 87–98. https://doi.org/10.1016/j.oregeorev.2013.04.010

Mukherjee, I. and Large, R., 2017. Application of pyrite trace element chemistry to exploration for SEDEX style Zn-Pb deposits: McArthur Basin, Northern Territory, Australia; Ore Geology Reviews, v. 81, p. 1249–1270. https://doi.org/10.1016/j.oregeorev.2016.08.004

Nadeau, O., Williams-Jones, A.E., and Stix, J., 2010. Sulphide magma as a source of metals in arc-related magmatic hydrothermal ore fluids; Nature Geoscience, v. 3, p. 501–505. https://doi.org/10.1038/ngeo899

Nimis, P., Zaykov, V.V., Omenetto, P., Melekestseva, I.Y., Tesalina, S.G., and Orgeval, J.J., 2008. Peculiarities of some mafic–ultramafic- and ultramafic-hosted massive sulfide deposits from the Main Uralian fault zone, southern Urals; Ore Geology Reviews, v. 33, no. 1, p. 49–69. https://doi.org/10.1016/j.oregeorev.2006.05.010

Ohmoto, H., 1996. Formation of volcanogenic massive sulfide deposits: the Kuroko perspective; Ore Geology Reviews, v. 10, p. 135–177. https://doi.org/10.1016/0169-1368(95)00021-6

Orchard, M.J., 1986. Conodonts from Western Canadian chert: their nature, distribution and stratigraphic application; *in* Conodonts: investigative techniques and applications, (ed.) R.L. Austin; Ellis Horwood Ltd. for British Micropaleontological Society, Chichester, England, p. 94–119.

Patten, C.G.C., Pitcairn, I.K., Alt, J.C., Zack, T., Lahaye, Y., Teagle, D.A.H., and Markdahl, K., 2019. Metal fluxes during magmatic degassing in the oceanic crust: sulfide mineralisation at ODP site 786B, Izu-Bonin forearc; Mineralium Deposita, v. 55, p. 469–489. https://doi.org/10.1007/s00126-019-00900-9

Pedersen, R.B., Rapp, H.T., Thorseth, I.H., Lilley, M.D., Barriga, F.J., Baumberger, T., Flesland, K., Fonseca, R., Fruh-Green, G. L., and Jorgensen, S. L., 2010. Discovery of a black smoker vent field and vent fauna at the Arctic Mid-Ocean Ridge; Nature Communications, v. 1, no. 1, p. 126. https://doi.org/10.1038/ncomms1124

Peter, J.M., 1992. Comparative geochemical studies of the Upper Triassic Windy Craggy and modern Guaymas Basin deposits: a contribution to the understanding of massive sulfide formation in volcano-sedimentary environments; Ph.D. thesis, University of Toronto, Toronto, Ontario, 562 p.

Peter, J.M., Leybourne, M.I., Scott, S.D., and Gorton, M.P., 2014. Geochemical constraints on the tectonic setting of basaltic host rocks to the Windy Craggy Cu-Co-Au massive sulphide deposit, northwestern British Columbia; International Geology Review, v. 56, p. 1484–1503. https://doi.org/10.1080/00206814.2014.947335

Peter, J.M. and Scott, S.D., 1988. Mineralogy, composition, and fluid-inclusion microthermometry of seafloor hydrothermal deposits in the southern trough of Guaymas Basin, Gulf of California; Canadian Mineralogist, v. 26, p. 567–587.

Peter, J.M. and Scott, S.D., 1999. Windy Craggy, northwestern British Columbia: the world's largest Besshi-type deposit, *in* Volcanic-associated massive sulfide deposits: processes and examples in modern and ancient settings, (ed.) C.T. Barrie and M.D. Hannington; Society of Economic Geologists, Reviews in Economic Geology, v. 8, p. 261–295.

Petrus, J.A., Chew, D.M., Leybourne, M.I., and Kamber, B.S., 2017. A new approach to laser-ablation inductively-coupled-plasma mass-spectrometry (LA-ICP-MS) using the flexible map interrogation tool 'Monocle'; Chemical Geology, v. 463, p. 76–93. https://doi.org/10.1016/j.chemgeo.2017.04.027

Reeves, E.P., Seewald, J.S., Saccocia, P., Bach, W., Craddock, P.R., Shanks, W.C., Sylva, S.P., Walsh, E., Pichler, T., and Rosner, M., 2011. Geochemistry of hydrothermal fluids from the PACMANUS, Northeast Pual and Vienna Woods hydrothermal fields, Manus Basin, Papua New Guinea; Geochimica et Cosmochimica Acta, v. 75, no. 4, p. 1088–1123. https://doi.org/10.1016/j.gca.2010.11.008

Richards, J.P., 2011. Magmatic to hydrothermal metal fluxes in convergent and collided margins; Ore Geology Reviews, v. 40, p. 1–26. https://doi.org/10.1016/j.oregeorev.2011.05.006

Rubin, K., 1997. Degassing of metals and metalloids from erupting seamount and mid-ocean ridge volcanoes: observations and predictions; Geochimica et Cosmochimica Acta, v. 61, p. 3525–3542. https://doi.org/10.1016/S0016-7037(97)00179-8

Saintilan, N.J., Creaser, R.A. and Bookstrom, A.A., 2017. Re-Os systematics and geochemistry of cobaltite (CoAsS) in the Idaho cobalt belt, Belt-Purcell Basin, USA: evidence for middle Mesoproterozoic sediment-hosted Co-Cu sulfide mineralization with Grenvillian and Cretaceous remobilization; Ore Geology Reviews, v. 86, p. 509–525. https://doi.org/10.1016/j.oregeorev.2017.02.032

Schmidt, K., Garbe-Schönberg, D., Hannington, M.D., Anderson, M.O., Bühring, B., Haase, K., Haruel, C., Lupton, J., and Koschinsky, A., 2017. Boiling vapour-type fluids from the Nifonea vent field (New Hebrides Back-Arc, Vanuatu, SW Pacific): geochemistry of an early-stage, post-eruptive hydrothermal system; Geochimica et Cosmochimica Acta, v. 207, p. 185–209. https://doi.org/10.1016/j.gca.2017.03.016

Schmidt, M.A., Leybourne, M.I., Peter, J.M., Petts, D., and Layton-Matthews, D., 2019. Fluid inclusion LA-ICP-MS and whole rock geochemical investigation of possible magmatic contributions to the giant Windy Craggy Besshi-type VMS deposit; *in* Targeted Geoscience Initiative: 2018 report of activities, (ed.) N. Rogers, Geological Survey of Canada, p. 189–204. https://doi.org/10.4095/313651

Schmidt, M.A., Peter, J.M., Jackson, S.E., Yang, Z., Leybourne, M.I., and Layton-Mathews, D., 2018. Laser ablation-inductively coupled plasma-mass spectro- metric analysis of fluid inclusions from the Windy Craggy Cu-Co-Au volcanogenic massive sulphide deposit: method development and preliminary results; *in*: Targeted Geoscience Initiative: 2017 report of activities, (ed.) N. Rogers, p. 243–252. https://doi.org/10.4095/306480

Sillitoe, R.H., 2010. Porphyry copper systems; Economic Geology, v. 105, no. 1, p. 3–41. https://doi.org/10.2113/gsecongeo.105.1.3

Slack, J.F., Kimball, B.E., and Shedd, K.B., 2017. Cobalt; Chapter F *in* Critical mineral resources of the United States—Economic and environmental geology and prospects for future supply, (ed.) K.J. Schulz, J.H. DeYoung Jr., R.R. Seal II, and D.C. Bradley; United States Geological Survey, Professional Paper 1802, p. F1–F40. https://doi.org/10.3133/pp1802F

Soltani Dehnavi, A., McFarlane, C.R.M., Lentz, D.R., and Walker, J.A., 2018. Assessment of pyrite composition by LA-ICP-MS techniques from massive sulfide deposits of the Bathurst Mining Camp, Canada: from textural and chemical evolution to its application as a vectoring tool for the exploration of VMS deposits; Ore Geology Reviews, v. 92, p. 656–671. https://doi.org/10.1016/j.oregeorev.2017.10.010

Sun, S.-s. and McDonough, W.F., 1989. Chemical and isotopic systematics of oceanic basalts: implications for mantle composition and processes; *in* Magmatism in the Ocean Basins, (ed.) A.D. Saunders and M.J. Norry; The Geological Society, Special Publication No. 42, p. 313–345.

Timm, C., de Ronde, C.E.J., Leybourne, M.I., Layton-Matthews, D., and Graham, I.J., 2012. Sources of chalcophile and siderophile elements in kermadec arc lavas; Economic Geology, v. 107, no. 8, p. 1527–1538. https://doi.org/10.2113/econgeo.107.8.1527

Timm, C., Leybourne, M.I., Hoernle, K., Wysoczanski, R.J., Hauff, F., Handler, M., Caratori Tontini, F., and de Ronde, C.E.J., 2016. Trench-perpendicular geochemical variation between two adjacent Kermadec arc volcanoes Rumble II East and West: the role of the subducted Hikurangi Plateau in element recycling in arc magmas; Journal of Petrology, v. 57, no. 7, p. 1335–1360. https://doi.org/10.1093/petrology/egw042

Villemant, B., Jaffrezic, H., Joron, J.-L., and Treuil, M., 1981. Distribution coefficients of major and trace elements; fractional crystallization in the alkali basalt series of Chaîne des Puys (Massif Central, France); Geochimica et Cosmochimica Acta, v. 45, no. 11, p. 1997–2016. https://doi.org/10.1016/0016-7037(81)90055-7

Volesky, J.C., Leybourne, M.I., Stern, R.J., Peter, J.M., Layton-Matthews, D., Rice, S., and Johnson, P.R., 2017. Metavolcanic host rocks, mineralization, and gossans of the Shaib al Tair and Rabathan volcanogenic massive sulphide deposits of the Wadi Bidah Mineral District, Saudi Arabia; International Geology Review, v. 59, p. 1975–2002. https://doi.org/10.1080/00206814.2017.1307789

Wilson, S.A., Ridley, W.I., and Koenig, A.E., 2002. Development of sulfide calibration standards for the laser ablation inductively-coupled plasma mass spectrometry technique; Journal of Analytical Atomic Spectrometry, v. 17, p. 406–409. https://doi.org/10.1039/B108787H

Wohlgemuth-Ueberwasser, C.C., Viljoen, F., Petersen, S., and Vorster, C., 2015. Distribution and solubility limits of trace elements in hydrothermal black smoker sulfides: an in-situ LA-ICP-MS study; Geochimica et Cosmochimica Acta, v. 159, p. 16–41. https://doi.org/10.1016/j.gca.2015.03.020

Wysoczanski, R.J., Handler, M.R., Schipper, C.I., Leybourne, M.I., Creech, J., Rotella, M.D., Nichols, A.R.L., Wilson, C.J.N., and Stewart, R.B., 2012. The tectonomagmatic source of ore metals and volatile elements in the Southern Kermadec Arc; Economic Geology, v. 107, p. 1539–1556. https://doi.org/10.2113/econgeo.107.8.1539

Yang, K.H. and Scott, S.D. (1996) Possible contribution of a metal-rich magmatic fluid to a sea-floor hydrothermal system; Nature, vol. 383, p. 420–423. https://doi.org/10.1038/383420a0

Yang, K.H. and Scott, S.D., 2006. Magmatic fluids as a source of metals in seafloor hydrothermal systems; *in* Back-arc spreading systems: geological, biological, chemical, and physical interactions, (ed.) D.M. Christie, C.R. Fisher, S.-M. Lee, S. Givens; Geophysical Monograph Series, Volume 166, p. 163–184.

Yeats, C.J., Parr, J.M., Binns, R.A., Gemmell, J.B., and Scott, S.D., 2014. The SuSu Knolls hydrothermal field, Eastern Manus Basin, Papua New Guinea: an active submarine high-sulfidation copper-gold system; Economic Geology, v. 109, p. 2207–2226.